2007

Soliton Solutions Of Nonlinear Partial Differential Equations Using Variational Approximations And Inverse Scattering Techniques

Thomas Vogel
University of Central Florida

SOLITON SOLUTIONS OF NONLINEAR PARTIAL DIFFERENTIAL EQUATIONS USING VARIATIONAL APPROXIMATIONS AND INVERSE SCATTERING TECHNIQUES

by

THOMAS K. VOGEL
B.S. University of Central Florida, 2000
B.S. University of Central Florida, 2000
M.S. University of Central Florida, 2001

A dissertation submitted in partial fulfillment of the requirements
for the degree of Doctor of Philosophy
in the Department of Mathematics
in the College of Sciences
at the University of Central Florida
Orlando, Florida

Summer Term
2007

Major Professor: David J. Kaup

ABSTRACT

Throughout the last several decades many techniques have been developed in establishing solutions to nonlinear partial differential equations (NPDE). These techniques are characterized by their limited reach in solving large classes of NPDE. This body of work will study the analysis of NPDE using two of the most ubiquitous techniques developed in the last century. In this body of work, the analysis and techniques herein are applied to unsolved physical problems in both the fields of variational approximations and inverse scattering transform. Additionally, a new technique for estimating the error of a variational approximation is established. Note that the material in chapter 2, "Quantitative Measurements of Variational Approximations" has recently been published [20].

Variational problems have long been used to mathematically model physical systems. Their advantage has been the simplicity of the model as well as the ability to deduce information concerning the functional dependence of the system on various parameters embedded in the variational trial functions. However, the only method in use for estimating the error in a variational approximation has been to compare the variational result to the exact solution. In this work, it is demonstrated that one can computationally obtain estimates of the errors in a one-dimensional variational approximation, without any *a priori* knowledge of the exact solution. Additionally, this analysis can be done by using only linear techniques. The extension of this method to multidimensional problems is clearly possible, although one could expect that additional difficulties would arise.

One condition for the existence of a localized soliton is that the propagation constant

does not fall into the continuous spectrum of radiation modes. For a higher order dispersive systems, the linear dispersion relation exhibits a multiple branch structure. It could be the case that in a certain parameter region for which one of the components of the solution has oscillations (i.e., is in the continuous spectrum), there exists a discrete value of the propagation constant, k_{ES}, for which the oscillations have zero amplitude. The associated solution is referred to as an embedded soliton (ES). This work examines the ES solutions in a $\chi^{(2)} : \chi^{(3)}$, type II system. The method employed in searching for the ES solutions is a variational method recently developed by Kaup and Malomed [Phys. D **184**, 153-61 (2003)] to locate ES solutions in a SHG system. The variational results are validated by numerical integration of the governing system.

A model used for the 1-D longitudinal wave propagation in microstructured solids is a KdV-type equation with third and fifth order dispersions as well as first and third order nonlinearities. Recent work by *Ilison* and *Salupere* (2004) has identified certain types of soliton solutions in the aforementioned model. The present work expands the known family of soliton solutions in the model to include *embedded solitons*. The existence of embedded solitons with respect to the dispersion parameters is determined by a variational approximation. The variational results are validated with selected numerical solutions.

TABLE OF CONTENTS

LIST OF FIGURES

LIST OF TABLES

INTRODUCTION

Throughout the last several decades many techniques have been developed in establishing solutions to nonlinear partial differential equations (NPDE). These techniques are characterized by their limited reach in solving large classes of NPDE. This body of work will study the analysis of NPDE using the idea of a Lagrangian formulation. Consider a nonlinear partial differential operator (NPDO), Λ, for which there exists some u such that

$$\Lambda[u] = 0 \tag{1.1}$$

Depending on the structure of Λ, solutions to equation (1.1) most likely cannot be found directly. In fact, it is difficult to make any generalization about (1.1) without imposing further structure on Λ. Instead of restricting Λ to a certain class of NPDO, consider a paradigmatic reformulation of (1.1). Suppose this nonlinear operator is the "derivative" of some associated "energy" functional, E.

$$\Lambda[u] = \nabla(E[u]) \tag{1.2}$$

Equation (1.1) may now be written as

$$\nabla(E[u]) = 0 \tag{1.3}$$

This establishes a duality in which solutions to equation (1.1) may be equivalently recognized as the critical points of the functional, $E[\bullet]$.

1.1 Variational Formalisms: First Principles

Definition 1.1.1 (Lagrangian) *Suppose $D \subset R^{\mathrm{n}}$ is a bounded, open set with boundary ∂D. The **Lagrangian** is a smooth functional*

$$L : \mathcal{R}^{\mathrm{n}} \times \mathcal{R} \times \overline{\mathrm{D}} \to \mathcal{R} \tag{1.4}$$

where $\overline{D} = D \cup \partial D$.

More specifically, the Lagrangian may be written as

$$L = L(\nabla u(x), u(x), x) \tag{1.5}$$

With this notation, the energy function described in (1.2) may be more explicitly written as

$$E[u] = \int_D L(\nabla u, u, x) dx \tag{1.6}$$

for smooth functions $u : D \to \mathcal{R}$ satisfying the boundary condition

$$u(x) = g \quad on \quad \partial D \tag{1.7}$$

Theorem 1.1.1 *Suppose u is a smooth function satisfying the boundary condition $u = g$ on ∂D. Further, assume u is a minimizer of $E[\bullet]$. Then u is a solution of a certain differential equation.*

Proof: Choose some smooth function $p(x) \in C^{\infty}(D)$ which is defined on compact support. Consider the real-valued auxiliary function given by

$$\tilde{E}(\epsilon) = E(u + \epsilon p) \quad for \;\; \epsilon \in \mathcal{R} \tag{1.8}$$

Since u is a minimizer, $\tilde{E}$ has a minimum at $\epsilon = 0$. Thus $\tilde{E}'(0) = 0$. This derivative may be computed directly (i.e., the Gauteaux derivative). Given that

$$\tilde{E} = \int_{\mathcal{U}} L(\nabla u + \epsilon \nabla p, u + \epsilon p, x) dx \tag{1.9}$$

the first variation is computed to be

$$\tilde{E}' = \int_D \sum_{j=1}^{n} L_{\nabla u_j}(\nabla u + \epsilon \nabla p, u + \epsilon p, x) p_{x_i} + L_u(\nabla u + \epsilon \nabla p, u + \epsilon p, x) p dx \tag{1.10}$$

Taking $\epsilon = 0$

$$0 = \tilde{E}'(0) = \int_\Omega \sum_{j=1}^{n} L_{\nabla u_j}(\nabla u, u, x) p_{x_i} + L_u(\nabla u, u, x) p dx \tag{1.11}$$

Since $p(x)$ has compact support, equation (1.11) can by integrated by parts to give

$$0 = \int_{\mathcal{U}} \left[-\sum_{j=1}^{n} (L_{\nabla u_j}(\nabla u, u, x))_{x_i} + L_u(\nabla u, u, x) \right] p(x) dx \tag{1.12}$$

This is true for any test function $p(x)$, and hence u must satisfy the differential equation

$$-\sum_{j=1}^{n} (L_{\nabla u_j}(\nabla u, u, x))_{x_i} + L_u(\nabla u, u, x) = 0 \tag{1.13}$$

This is the *Euler-Lagrange* equation associated with the energy functional defined in equation (1.2). The result is that solutions to (3.23) may be sought as minimizers of (1.6).

1.2 Existence and Uniqueness of Minimizers

This section will address the conditions under which $E[\bullet]$ should have a minimizer. To begin, recognize that a smooth mapping $f : \mathcal{R} \to \mathcal{R}$ bounded from below need not attain its infimum. For example, consider $f(x) = e^{-x^2}$. It is bounded from below, but $f(x) \neq inf[f(x)]$ for any $x \in \mathcal{R}$. One way to ensure a function which is bounded from below will achieve it's infimum is to assume that $|f| \to +\infty$ whenever $|x| \to \infty$. There arises a need to create a controlling mechanism for $E[u]$, when u is a "large" function.

Condition 1.2.1 (Coercivity) *Fix p such that $1 < p < \infty$. Further, suppose that there exists $\alpha > 0$ and $\beta \geq 0$ such that*

$$L(\nabla u, u, x) \geq \alpha |\dot{u}|^p - \beta, \quad for \quad all \quad \dot{u} \in \mathcal{R}^n, \quad u \in \mathcal{R}, \quad and \quad x \in D \tag{1.14}$$

*Then the **coercivity** condition on $E[\bullet]$ is given by*

$$E[u] \geq \alpha \int_D |\nabla u|^p dx - \beta |D|_{max} \tag{1.15}$$

Notice that from the above condition,

$$E[u] \to \infty \ \ as \ \ \int_D |\nabla u|^p dx \to \infty \tag{1.16}$$

The class of functions for which minimizer candidates arise need not be smooth. This condition can be relaxed so as to include functions in the Sobolev space $W^{1,p}(D)$. The class of admissible functions through which a minimizer is sought will be taken to be:

$$\mathcal{A} = \{u \in W^{1,p}(\Omega) | u = g \ \ on \ \ \partial D\} \tag{1.17}$$

Theorem 1.2.1 (Existence of minimizer) *Assume that L satisfies the coercivity condition and is convex in ∇u. Suppose further that the admissible $\mathcal{A}$ set is nonempty. Then there exists at least one function $u \in \mathcal{A}$ solving*

$$E[u] = min_{w \in \mathcal{A}} E[w] \tag{1.18}$$

Theorem 1.2.2 (Uniqueness of minimizer) *Suppose $L = L(\nabla u, x)$ does not depend on $u(x)$. Further, suppose that the mapping $\nabla u \rightarrow L(\nabla u, x)$ is uniformly convex for each $x \in \mathcal{R}$. Then a minimizer $u \in \mathcal{A}$ of $E[\bullet]$ is unique.*

Proofs of the above two theorems are presented in [10].

1.3 Variational Approximation of the Equations of Motion

Variational problems have existed in mathematics throughout history. One such classical example is: given a fixed perimeter, what geometry encloses the largest area? To have the ability to posture dynamic physical systems as a variational problem is quite intriguing. It means that the evolution of the system moves in such a way as to minimize or maximize something. More specifically, it moves in such a way as to minimize the action

$$S = \int_a^b L(x, u, u_x) dx \tag{1.19}$$

This lends to the Lagrangian some physical significance. As Richard Feynman points out "it is as though the system feels out the action on many possible paths and chooses the one for which the action is minimal". In fact, the question arises as to which quantity is more fundamental: the Lagrangian or the equations of motion. In practice, there are times

in which the Lagrangian is first established through various considerations. It is only an afterthought that a variational technique is employed to establish the equations of motion for which the Lagrangian represents. To further this point, establishing the Lagrangian from the equations of motion is an *inverse problem* in mathematics.

One of the purposes of this work is to develop variational techniques that can be employed to reverse engineer physical systems. The modality of this paradigm is quite simple. Suppose the Lagrangian, L, corresponding to some physical system is known. Define the operator Λ to be the first variation:

$$\Lambda[\bullet] = \frac{\delta L[\bullet]}{\delta u} \tag{1.20}$$

The equations of motion can then be obtained from L. They are determined by

$$\Lambda[u] = 0 \tag{1.21}$$

Suppose that the exact solution, $u = u_e$, of (2.4) is unknown. Express this solution in terms of some reasonable "guess" trial function, plus some error correction term.

$$u_e = g + h \tag{1.22}$$

One goal is to establish an error bound on h exclusively in terms of the guess function g. Suppose the trial function depends on some number of static parameters, μ_i. (This is a simplifying assumption. In general the parameters could evolve in a non-algebraic manner). For example, suppose there is some suspicion that a localized soliton solution may exist for

some physical system. The trial function could then be defined in terms of a width, position, velocity, chirp, and phase. From the Lagrangian, the action can be established according to

$$S = \int_{\partial D} L[u_e] dt \tag{1.23}$$

A set of Euler-Lagrange equations may then be established in terms of the various parameters. These E-L equations will evolve according to

$$\frac{\delta S}{\delta \mu_i} = 0 \tag{1.24}$$

In the case of static parameters (i.e., μ_i are constant), then the functional derivative reduces to a partial derivative:

$$\frac{\partial S}{\partial \mu_i} = 0 \tag{1.25}$$

Substituting the ansatz given by (1.22) into (2.1) yields:

$$\begin{aligned} S &= \int_{\partial D} L[u_e] dt = \int_{\partial D} L[g+h] dt \\ &= \int_{\partial D} L[g] dt + \int_{\partial D} \frac{\delta L[g]}{\delta u} h dt + \frac{1}{2} \int_{\partial D} \int_{\partial \tilde{D}} \frac{\delta^2 L[g]}{\delta u \delta \tilde{u}} h \tilde{h} dt d\tilde{t} + O(h^3) \end{aligned} \tag{1.26}$$

Utilizing condition (1.25), this may be rewritten as

$$\int_{\partial D} \frac{\partial L[g]}{\partial \mu_i} dt + \int_{\partial D} \frac{\partial \Lambda[g]}{\partial \mu_i} h dt + \int_{\partial D} \Lambda[g] \frac{\partial h}{\partial \mu_i} dt + O(h^2) = 0 \tag{1.27}$$

Integrating this result by parts (with respect to t) produces

$$\int_{\partial D} \frac{\partial L[g]}{\partial \mu_i} dt + h|_{t\in\partial D} \int_{\partial D} \frac{\partial \Lambda[g]}{\partial \mu_i} dt + \frac{\partial h}{\partial \mu_i}|_{t\in\partial D} \int_{\partial D} \Lambda[g] dt \tag{1.28}$$
$$- \int_{\partial D} \left(\int_{\partial \tilde{D}} \frac{\partial \Lambda[g]}{\partial \mu_i} d\tilde{t} \right) \frac{dh}{dt} dt - \int_{\partial D} \left(\int_{\partial \tilde{D}} \Lambda[g] d\tilde{t} \right) \frac{\partial^2 h}{\partial \mu_i dt} dt + O(h^2) = 0$$

Suppose that $h(t;\mu_i)$ attains its maximum on $t \in \partial D$. Then (1.28) implies that

$$\left(\int_{\partial D} \Lambda[g] dt \right) \frac{\partial h_{max}}{\partial \mu_i} + \left(\int_{\partial D} \frac{\partial \Lambda[g]}{\partial \mu_i} dt \right) h_{max} = - \int_{\partial D} \frac{\partial L[g]}{\partial \mu_i} dt + O(h^2) \tag{1.29}$$

Notice that the error, $h(t)$, propagates according to linear perturbation theory. The solution for the linearized equation (i.e. lowest order in h) is given by

$$h_{max} = M \exp\left(- \int \frac{\int_{\partial D} \frac{\partial \Lambda[g]}{\partial \mu_i} dt}{\int_{\partial D} \Lambda[g] dt} d\mu_i \right) \int \left(\frac{\int_{\partial D} \frac{\partial L[g]}{\partial \mu_i} dt}{\int_{\partial D} \Lambda[g] dt} \right) \exp\left(- \int \frac{\int_{\partial D} \frac{\partial \Lambda[g]}{\partial \mu_i} dt}{\int_{\partial D} \Lambda[g] dt} d\mu_i \right) d\mu_i|_{t=t_{max}} \tag{1.30}$$

Note that $lim_{g\to u} h_{max}$ is singular. The importance of the above bound may be more theoretically important than it is computationally useful. It demonstrates that it is possible to obtain a gauge for the error correction, h, exclusively in terms of the trial function, g. This idea is developed fully in chapter 2, and has recently been published [20].

Given the evolution of some physical system, represented by the operator $\Lambda[\bullet]$, how can one "measure" the accuracy of the variational approximation? What other quantities exist that will allow for a "gauge" on the error function h? The variational principle yields the Euler-Lagrange equations not simply when the action is a minimum, but more generally when its derivative vanishes. This could correspond to a minimum, maximum, or a saddle point. To determine which it is requires an examination of the quantity:

$$\delta^2 S = \frac{d^2}{d\epsilon^2} S(u + \epsilon p)|_{\epsilon=0} \tag{1.31}$$

For all admissible test functions, $p(x)$. This quantity can be interpreted as the curvature of the action. For the action to be a minimum, it is required that

$$\delta^2 S \geq 0 \tag{1.32}$$

It has been shown (Gel'fand and Fomin 1963) that a necessary, but not sufficient condition for this is given by

$$\frac{\partial^2 L}{\partial u_x \partial u_x} \geq 0 \tag{1.33}$$

As an example, consider varying

$$S = \int_a^b L(x, u, u_x) dx \tag{1.34}$$

Choose some test function $p(x) \in C^2[a, b]$ such that p vanishes along the boundary. The second variation is then determined by

$$\delta^2 S = \frac{d^2}{d\epsilon^2} S(u + \epsilon p)|_{\epsilon=0} \tag{1.35}$$

In terms of the Lagrangian, (1.35) is

$$\frac{d^2}{d\epsilon^2} S(u + \epsilon p)|_{\epsilon=0} = \int_a^b [L_{uu} p^2 + 2L_{u_x u} h \frac{dp}{dx} + L_{u_x u_x} (\frac{dp}{dx})^2] dx \tag{1.36}$$

Integration by parts leads to an expression for the second variation given by

$$\int_a^b \{[p^2[L_{uu} - \frac{d}{dx}L_{u_x u} + \frac{1}{2}\frac{d^2}{dx^2}L_{u_x u_x}] + p\frac{d^2 h}{dx^2}L_{u_x u_x}\}dx \tag{1.37}$$

An important note here is that the second variation depends on the test function. This is not the case for the first variation. The curvature of the action represents a real positive definite quantity.

1.4 A Variational Approximation of the Vibrating String

To illustrate these ideas, consider the following example using the linear wave equation.

$$\partial_t^2 u(x,t) = \alpha^2 \partial_x^2 u(x,t) \quad 0 \le x \le 4a \quad 0 \le t < \infty \tag{1.38}$$

subject to

$$\text{B.C.'s: } u(0,t) = 0 \quad u(4a,t) = 0$$

$$\text{I.C.'s: } u(x,0) = f(x) \quad \partial_t u(x,0) = y(x)$$

The above PDE is solved by

$$u(x,t) = \sum_{n=1}^{\infty} \sin(\frac{n\pi x}{4a})[a_n \sin(\frac{n\pi\alpha t}{4a}) + b_n \cos(\frac{n\pi\alpha t}{4a})] \tag{1.39}$$

where

$$a_n = \frac{2}{n\pi\alpha}\int_0^L g(x) sin(\frac{n\pi x}{4a})dx \tag{1.40}$$

$$b_n = \frac{1}{2a}\int_0^L f(x) sin(\frac{n\pi x}{4a})dx \tag{1.41}$$

Consider the operator

$$L(\partial_x, \partial_t)[\bullet] = \frac{1}{2}\left(\alpha^2 |\partial_x[\bullet]|^2 - |\partial_t[\bullet]|^2\right) \tag{1.42}$$

In terms of this operator, equation (1.38) may be written as

$$\frac{\delta L[u]}{\delta u} = 0 \tag{1.43}$$

Now a variational approximation will be employed to estimate the accuracy of a geometric model with respect to the equation of motion (for the vibrating string). The solution is essentially characterized by the phase of the oscillation. While the exact solution is a superposition of an infinite number of Fourier modes; the approximation will be tested against a single mode. More specifically, the second mode. Consider the function

$$g(x,t;a,b(t)) = \begin{cases} \frac{b}{a}x & 0 \le x < a \\ -\frac{b}{a}x + 2b & a \le x < 3a \\ \frac{b}{a}x - 4b & 3a \le x < 4a \end{cases} \qquad where \;\; a, b(t) \in \mathcal{R} \tag{1.44}$$

Which is periodic with $P = 4a$.

To estimate how far this is from the exact second harmonic, a variational formulation will be utilized. The parameter a is fixed at the endpoints of the vibrating string, and $b = b(t)$. The action integral is then given by

$$S(t;a,b(t)) = \int_0^{4a} L[g, g_x, g_t]dx \tag{1.45}$$

Which is evaluated to be

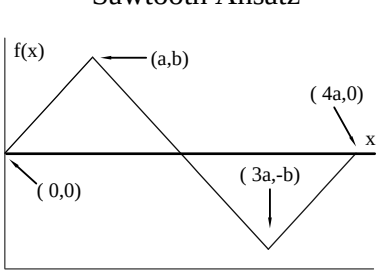

Figure 1.1: sawtooth variational ansatz for the vibrating string

$$2\,\frac{\alpha^2\left(b\left(t\right)\right)^2}{a}-2/3\,\left(\frac{d}{dt}b\left(t\right)\right)^2 a \tag{1.46}$$

Varying the action integral with respect to $b(t)$ yields the following results:

$$\frac{\delta b}{\delta t}=\frac{dS}{db(t)}-\frac{d}{dt}[\frac{dS}{db'(t)}]=4\,\frac{\alpha^2 b\left(t\right)}{a}+4/3\,\left(\frac{d^2}{dt^2}b\left(t\right)\right)a=0 \tag{1.47}$$

The solution to equation (1.47) is given by

$$b\left(t\right)=C_1\sin\left(\frac{\sqrt{3}\alpha\,t}{a}\right)+C_2\cos\left(\frac{\sqrt{3}\alpha\,t}{a}\right) \tag{1.48}$$

Next consider a parabolic approximation to the second harmonic of the vibrating string:

$$g(x,t)=\begin{cases}-\frac{b}{a^2}(x-a)^2+b & 0\le x<2a\\ \frac{b}{a^2}(x-3a)^2-b & 2a\le x<4a\end{cases}\qquad where\ \ a,b(t)\in\mathcal{R} \tag{1.49}$$

The action is computed to be

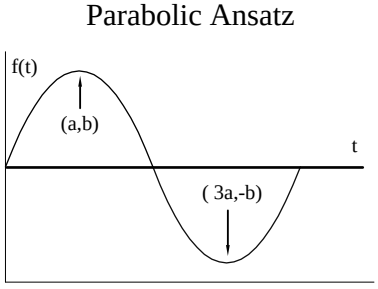

Figure 1.2: parabolic variational ansatz for the vibrating string

$$
\begin{aligned}
S &= \frac{1008}{5}\left(\frac{d}{dt}b\left(t\right)\right)^{2}a+8/3\left(2\frac{\alpha^{2}\left(b\left(t\right)\right)^{2}}{a^{4}}-2\frac{\left(\frac{d}{dt}b\left(t\right)\right)^{2}}{a^{2}}\right)a^{3}+32\frac{\alpha^{2}\left(b\left(t\right)\right)^{2}}{a} \qquad (1.50)\\
&+ \frac{56}{3}\left(2\frac{\alpha^{2}\left(b\left(t\right)\right)^{2}}{a^{4}}-26\frac{\left(\frac{d}{dt}b\left(t\right)\right)^{2}}{a^{2}}\right)a^{3}+6\left(-12\frac{\alpha^{2}\left(b\left(t\right)\right)^{2}}{a^{3}}+48\frac{\left(\frac{d}{dt}b\left(t\right)\right)^{2}}{a}\right)a^{2}=0
\end{aligned}
$$

The evolution of $b(t)$ is then determined by:

$$\frac{\delta b}{\delta t}=16/3\frac{\alpha^{2}b\left(t\right)}{a}+\frac{32}{15}\left(\frac{d^{2}}{dt^{2}}b\left(t\right)\right)a \qquad (1.51)$$

The solution to condition (1.51) is given by

$$b\left(t\right)=C_{1}\sin\left(1/2\frac{\sqrt{10}\alpha\,t}{a}\right)+C_{2}\cos\left(1/2\frac{\sqrt{10}\alpha\,t}{a}\right) \qquad (1.52)$$

Comparing these approximations to the second harmonic of the vibrating string indicates the following:

Exact temporal phase: $\frac{n\pi\alpha}{4a}$

Sawtooth temporal phase: $\frac{\sqrt{10}\alpha}{2a}\rightarrow n\approx 2.21$

Parabolic temporal phase: $\frac{\sqrt{3}\alpha}{a} \rightarrow n \approx 2.01$

The above result demonstrates the usage of a variational approximation to estimate solutions of a differential equation. The resulting accuracy of the variational approximation is obtained by comparsion to the exact solution. The next chapter establishes a new technique by which the accuracy of a variational approximation can be gauged without knowledge of the exact solution.

QUANTITATIVE APPROXIMATIONS OF VARIATIONAL APPROXIMATIONS

2.1 Introduction

In the theory of modern dynamics, there exist two paradigmatic views on formulating the mathematical model for a physical system. These paradigms arrive at a completely equivalent result. The first perspective, commonly viewed as the Newtonian approach, argues that the evolution of the state of a process can be completely described in terms of the *forces* involved with the process. This approach is a manifestation of the Aristotelian "cause and effect" view of the universe. The mathematical framework for the second perspective is based on two publications [11, 12] in the 1830's by William Hamilton. Within these papers, Hamilton proposes a theory of dynamics which describes all of classical (Newtonian) mechanics *without the use of forces*. Instead, the physical process under consideration will evolve in such a way as to extremize the integral of the difference between the kinetic and potential energies. Philosophically, this is in stark contrast to the Newtonian perspective. Instead of viewing the evolution of a process as a result of external influences, the Hamiltonian approach suggests there is an *internal intention* on the part of the process to evolve in a particular manner.

Variational problems have existed in mathematics throughout history. The earliest that we have located was in the *Aeneid* [13], where there is a legend of a woman who fled to Africa after her husband was murdered. She arrived somewhere along the North African coast where she pleaded with the local ruler, King Jambus, for land. The King granted the

woman as much land as could be enclosed with the hide of a bull. Legend says that she cut the hide into very thin and long strips, the land later became the city of Carthage (c. 814 BC) and the woman its ruler, Queen Dido. While legend and fact may not necessarily agree, this demonstrates that the idea of extremum principles have existed for millenia. About eight centuries later, Hero of Alexandria (c 10-70) proved the first recorded scientific minimum principle. He was able to show that the trajectory of a reflected light ray is a minimum if the angles of incidence and reflection are equal [21]. This idea was later formulated as a least time principle by Fermat in the early part of the seventeenth century [21].

The mathematical machinery necessary to investigate such problems was found to require more than the elementary calculus developed by Newton [26] and Leibniz in the mid-seventeenth century. In 1696, Johann Bernoulli proposed *"... brachistochrone problem which can be summarized as 'If two points are connected by a wire whose shape is given by an unknown function $y(x)$ in a vertical plane, what shape function minimizes the time of descent of a bead sliding withought friction from the higher to the lower point.'"*[25]. This problem was addressed by several of Bernoulli's contemporaries, and what arose from these investigations was a new type of calculus. This calculus is known today as the *calculus of variations* and was developed into a full mathematical theory by Euler around 1744 [4]. The mathematics developed by Euler was extended by Joseph-Louis Lagrange (1736-1813) . Lagrange discovered that Euler's equation for minimizing a functional integral (later to be named the Euler-Lagrange equation) could be expressed in a compact way by simply using integration by parts. It was Lagrange who introduced the integrand of the functional appropriate to mechanics, i.e., the difference between potential and kinetic energies. Euler had essentially

only considered the kinetic energy which amounted to requiring additional conditions to get a correct picture of classical mechanics [1].

Since the solution(s) of a dynamical system is one which extremizes this quantity called the action, it therefore follows from this principle that one can also devise methods for finding approximate solutions. Thus even if one reduces the number of degrees of freedom in which the function can be varied, Hamilton's Principle will lead one to a solution which, in some sense, will be as close as possible to the correct solution. However, due to the reduction in the number of degrees of freedom, one cannot generally expect the function to achieve the actual extremum of the full problem, but nevertheless, one can still expect to find an extremum, which should be "near" the exact solution. This method has long been used in applications from geometry [28] through quantum mechanics [22, 27]. In particular, it was in this period that we have the "Raleigh-Ritz method" being developed independently by Raleigh and Ritz[1], for finding eigenfunctions and eigenvalues of linear differential equations. This method is known in modern mathematical literature as the Raleigh-Ritz method [8, 3]. In fact this usage of variational methods continued into the first half of the 20th Century, and even up into the late 1980's. During this time, Quantum Mechanics and all of Modern Physics were born, and with these, there came a critical need to be able to obtain numerical values for comparing with experiments. Up until the 1950's, there were no electronic computers, and even in the latter half of the 20th, such electronic devices were generally only available at large

[1]The authors were not able to identify historical records of the work done by Raleigh and Ritz, only that the name of the method seemed to have been adopted sometime during the late 19thCentury, which was the time period in which Raleigh and Ritz performed their work.

government labs or universities, and ever there, their usage were quite limited. Otherwise, one only slide-rules or crude electric-operated mechanical calculators for use. Thus there was a definite need for methods for obtaining some kind of approximate solutions when one only had such devices. Whence the power of analytical methods of mathematics was put into use with these devices. As an answer to this need, there was major efforts to utilize variational methods for developing approximate solutions, as well as perturbation expansions of such, for various physical systems [24]. We note that in this time period, nonlinear problems were generally not studied as such, except to the degree that one could expand about some solvable linear problem, or some know analytical solution. Thus it is not surprising that all the work in this period mainly concentrated on linear eigenvalue problems and their perturbations, with variational methods playing leading roles. The need for this development of variational methods began to decline after the 1970's, with the increasing availability of calculators and computers, and particularly with the advent of the personal computer and the accompanying tremendous increase in computational power that came with these devices and their larger brothers. This marked the end of an era and the beginning of a new one. Within a decade, it would no longer be important to carefully and analytically expand solutions of equations of motion, in order to obtain a three-to-four place accuracy in their numerical values, when with the touch of a few keys, the value desired would appear almost instantly and with an 8-to-14 place accuracy.

Nevertheless, even though computations no longer needed to utilize variational methods, there has always been other usages of variational methods, in spite of the computational power that was now generally available. In particular, the variational methods have always

been adapt at providing functional dependences and trends, and thereby a single, simple variational result could contain more information than dozens of pages of numerical computations. For example, when a nonlinear problem contains three parameters and is also a differential system of twelveth-order, one would like to be able to localize as much as possible the parameter regime wherein one would need to search for soliton solutions. Such can indeed be done with variational methods [**?**]. Furthermore, variational techniques from numerical methods (such as the Galerkin method) have been used to develop variational methods for dissipative systems [16] and also to study the parameter space of electron devices [19]. Indeed, variational methods have been used to find approximate solutions in various cases, particularly in cases where closed-form solutions would not generally exist [**?**, 16, 17, 14, 15, 29]. However at the same time, variational methods can also lead to wrong or uncertain results [19, 15], and thus there is also a need for an even deeper and more through understanding of these methods. In particular, there is a need to be able to discern when a variational method is not "sufficiently close" to serve as an adequate approximation.

At this point, we probably should lay down a nomenclature for the terms that we have used above, and for new terms which will arise. By "Hamilton's Principle", we mean the general principle which states that the equations of motion of a conservative physical system are the Euler-Lagrange for the appropriate Lagrangian. By "variational method" we mean a method that makes use of a Hamilton's Principle in some manner. To distinguish the use of Hamilton's Principle for finding approximate solutions from other uses of variational methods, we shall refer to this use of Hamilton's Principle as the "Variational Approximation" (VA). We note that the Raleigh - Ritz method is also a VA, and which has been predomi-

nately used for linear eigenvalue problems. The term VA is intended to include applications to nonlinear systems as well. More general variational methods, such as those used in Ref. [16], should perhaps be called a "Gelerkin variational method", but we shall not directly discuss those methods here. However the reader should be aware that what we shall present here can easily be extended that method also.

The major criticism of any use of the VA has generally concentrated on the fact that there was no general method for estimating the quantitative validity of the VA, except by comparison with the exact solution, thereby requiring exact solutions anyway. With the VA, one has obtained an approximate solution. But how could one determine whether or not this approximate solution was of sufficient accuracy to be of value? In the absence of having the exact solution, one had no way to answer this. And this fact has always caused one to hesitate, even if only momentarily, before using or quoting variational results, in spite of its many frequent successes. Thus a method for the quantitative evaluation of any VA is needed.

As mentioned above, in the VA one expects to find a solution "close" to the exact solution. But how close is "close"? The key to determining this is to return to when variational methods were being intensely used, which was the early 20th Century, where even perturbation methods for VAs were being developed [24]. Certainly it would have been generally known that the size of a term at any one given order would give an estimate of the accuracy at that order. And certainly this would have been used to determine how many orders one needed to expand out to. At the same time, this also clearly tells us how to quantitatively estimate any VA. What has to be done, is to formulate the VA as

the leading term in a perturbation expansion. Then provided that one is expanding about a function which is sufficiently close to the exact solution, any term in the perturbation expansion will indicate the resulting error, if the series is terminated at that term. Note that here we are discussing functional accuracy, not numerical accuracy. This is a step higher than what was used in the Raleigh-Ritz method, wherein the criteria was only the accuracy of the eigenvalue. But at the same time, there is no one single number that can represent "functional accuracy". The purpose of this paper is to present such a method for *quantitatively* estimating the functional error in any VA, without knowing the exact solution, and by the use of only linear techniques. Then from the functional accuracy, be able to determine the numerical accuracy in any quantity of interest.

The method of the VA is quite straight-forward: establish the Lagrangian for the governing system, choose a reasonable trial function (ansatz) containing certain arbitrary parameters, calculate the action for that ansatz, and then determine the optimum parameters of the ansatz by solving the Euler-Lagrange equations which result from varying the action with respect to each parameter [2]. Then we will quantitatively estimate the error in the VA without using the exact solution. All that is required is for one to be able to solve a linear problem, to be defined below.

To illustrate this method, two physical systems will be analyzed. These systems are simple, so that the method can be easily illustrated. The first system is a vibrating string. Using a sawtooth ansatz and a parabolic ansatz, we will demonstrate how to quantitatively determine how "close" the VA is to the correct solution. The second model will be the well-known soliton solution of the Korteweg-de Vries (KdV) equation. Here we will use a

Guassian ansatz, and demonstrate how to quantitatively estimate two types of errors which this VA could introduce into another calculation. In one case, we will have the gaussian ansatz as being an acceptable approximation and in the other, as being unacceptable.

2.2 Theory

Let us first outline the theory behind this method of quantitatively estimating the error in a VA. Suppose the Lagrangian, L, corresponding to the physical system of interest is known, and that this Lagrangian is a functional of the variable $u(t)$. (The variable $u(t)$ may be a scalar, vector or tensor quantity.) For now, we shall only consider a one-dimensional scalar case, where the integration variable is t.

The action, $S[u]$, is define by:

$$S = \int_{\mathcal{D}} L[u]dt\,, \tag{2.1}$$

where $\mathcal{D}$ is the domain of support of the function u. Hamilton's Principle states that the governing equations of the variable $u(t)$ will be such that

$$\lim_{\epsilon\to 0} \frac{S[u(t)+\epsilon\delta u(t)] - S[u(t)]}{\epsilon} = \int_{\mathcal{D}} \frac{\delta L}{\delta u}[u(t)]\,\delta u(t)\,dt = 0\,, \tag{2.2}$$

for any bounded variation $\delta u(t)$, provided that this variation vanishes at any and all end points of the domain $\mathcal{D}$. Note that this also defines the quantity $\frac{\delta L}{\delta u}(t)$, which is called the (first) variational derivative of L.

Now, let us define the (nonlinear) operator Φ to be the first variational derivative of L:

$$\Phi[\bullet] = \frac{\delta L[\bullet]}{\delta u}\,. \tag{2.3}$$

This gives us the Euler-Lagrange equation,

$$\Phi[u_e] = 0\,, \tag{2.4}$$

where u_e will be the exact solution(s). (There could be more than one solution, depending on boundary conditions on u_e.) Thus the problem is to find u_e. Let us now use Hamilton's Principle to obtain a variational approximation to $u_e(t)$. The problem is then to find the "best" solution for whatever ansatz is chosen (the VA), and then to obtain a quantitative estimate of its resulting error(s).

As indicated above, we want to expand u_e in a perturbation expansion about the ansatz plus some error. Let $u_0(t;q)$ be the ansatz, where q is some finite collection of parameters, on which u_0 is dependent. Then we should expand u_e as

$$u_e = u_0(t;q) \,+\, \epsilon u_1(t) \,+\, \epsilon^2 u_2(t) \,+\, \ldots\,, \tag{2.5}$$

where here ϵ is an expansion parameter, whose size will be defined shortly. The collection of parameters, q, on which the trial function is dependent, are assumed to be finite and could include an amplitude, width, position, velocity, chirp, phase, etc., depending on the problem. The variation of u_0 will then consist only of the changes that occurs in u_0 when these parameters are varied. In varying these parameters, from (2.2), we will obtain a finite number of independent variations of S.

Let us see what this expansion can tell us. Substituting the expansion given by (2.5) into

(2.1), and then expanding about $u = u_0$, yields:

$$\begin{aligned} S &= \int_{\mathcal{D}} L[u_e]dt = \int_{\mathcal{D}} L[u_0 + \epsilon u_1 + \epsilon^2 u_2]dt\,, \\ &= \int_{\mathcal{D}} L[u_0]dt + \epsilon \int_{\mathcal{D}} \left(\frac{\delta L}{\delta u}\right)_0 (u_1 + \epsilon u_2)dt \\ &\quad + \epsilon^2 \frac{1}{2} \int_{\mathcal{D}} \int_{\tilde{\mathcal{D}}} \left(\frac{\delta^2 L}{\delta u(t)\delta u(t')}\right)_0 u_1(t)u_1(t')dtdt' + O(\epsilon^3)\,, \end{aligned} \tag{2.6}$$

where the subscript "0" indicates evaluation at $u = u_0$. Now consider the expression above. By Hamilton's Principle, we are to find a u_e such that for small variations about u_e, we will have $\delta S = 0$. In this variation, we shall vary the parameters q and the functions u_1, u_2, etc.

Consider the leading order term in Eq. (2.6). Since the functional form of u_0 has been fixed, we can only vary the parameters q. In lowest order ($\epsilon = 0$), variations of the q's will give the set of equations

$$\frac{\partial S}{\partial q} = \frac{\partial}{\partial q} \int_{\mathcal{D}} L[u_0]dt = 0\,, \tag{2.7}$$

which determine the lowest order solution (and structure) of the q's. Once this is done, we have the q's determined, which is the result of applying the VA.

Let us consider the next order, the ϵ term. By varying the function u_1 we can impose additional linearly independent variations, beyond what was imposed in zeroth order. Varying u_1 in the ϵ term will give us:

$$\left(\frac{\delta L}{\delta u}\right)_0 = 0\,, \tag{2.8}$$

which is nothing more than the equation(s) of motion evaluated at the ansatz ($u = u_0$). However, unless u_0 happens to be an exact solution, it is *impossible* for this condition to be satisfied. But it can be *almost* satisfied if u_0 is close to an exact solution, in which case the left hand side of (2.8) will actually be "small" but nonzero. And since it is nonzero, it must

be balanced by something. The only possible term that could balance it are the next higher order terms, which are the ϵ^2 terms in (2.6). This we can naturally do if we take the size of ϵ to be determined by the order of magnitude of $\left(\frac{\delta L}{\delta u}\right)_0$. So since (2.8) cannot generally be satisfied, we then must take

$$\left(\frac{\delta L}{\delta u(t)}\right)_0 = \epsilon R(t;q)[q]\,, \tag{2.9}$$

which defines R and at the same time also defines ϵ. Inserting (2.9) into (2.6) then gives us an expansion in which no ϵ terms are present. Rather, the next lowest order terms are the ϵ^2 terms and upon varying u_1 in these ϵ^2 terms, one obtains

$$\int_{\mathcal{D}} \left(\frac{\delta^2 L}{\delta u(t)\delta u(t')}\right)_0 u_1(t')dt' = -R(t)[q]\,. \tag{2.10}$$

Note that this equation is linear in u_1, and thus to determine u_1, one only has to solve a linear nonhomogeneous problem.

In hindsight, this result is not surprising. Although we have used Hamilton's Principle to derive this result, one just as easily could have derived it from the Euler-Lagrange equations. From (2.3) - (2.5), upon using (2.9), one can easily obtain (2.10). One can also interpret what is occurring here, and give an simple statement of its procedure. One starts with an ansatz, u_0, and uses the VA to calculate the best values for its parameters. Then we calculate the first-order correction to the ansatz, u_1, based on the *linearly perturbed* Euler-Lagrange equations, (2.10). The smallness of various features of this correction will be a basis for a quantitative measure of the validity of the VA.

2.3 The Vibrating String

The vibrating string of a finite length ℓ, fixed at both ends, has a simplicity which allows one to readily understand the approach used. If we decompose its evolution into normal modes, then we may use a VA to determine the modal shapes and the modal eigenfrequencies. The modal problem is a linear eigenvalue problem, with a well known solution. We take the Euler-Lagrange equation to be:

$$\Phi[u(x)] = 0\,; \quad \Phi[\bullet] = \frac{d^2}{dx^2}[\bullet] + k^2[\bullet]\,, \tag{2.11}$$

where $\Phi[\bullet]$ is the (linear) operator, k^2 is the eigenvalue, the interval is $[0 \leq x \leq \ell]$ and the integration variable is now changed to x. Our boundary conditions are $u(0) = 0 = u(\ell)$.

Since this problem is linear, the amplitude of the solution is arbitrary. To eliminate this irrelevant degree of freedom, we shall require the $\mathcal{L}^{(2)}$ norm of the eigenmode, $u(x)$, to be unity.

For the system described in (2.11), we may take the Lagrangian to be

$$L(u, u_x) = \frac{1}{2}\left(\frac{du}{dx}\right)^2 - \frac{1}{2}\nu u^2\,, \tag{2.12}$$

where $\nu = k^2$ is the eigenvalue. Note that due to translational invariance, we only need to treat the case of the fundamental mode, since the $n\underline{\text{th}}$-order mode for a string of length ℓ, can be obtained from the fundamental mode of a string of length ℓ/n.

2.3.1 The Variational Approximation

We shall consider two different approximations for the fundamental eigenfunction of (2.11): a sawtooth approximation and an upside-down parabola, each of which is given by:

$$u_0^{(sawtooth)}(x;A,\ell) = \begin{cases} \frac{2A}{\ell}x & 0 \le x < \frac{\ell}{2}\,, \\ \frac{2A}{\ell}(\ell - x) & \frac{\ell}{2} \le x < \ell\,, \end{cases} \tag{2.13}$$

$$u_0^{(parabolic)}(x;A,\ell) = A[1 - (\frac{2x}{\ell} - 1)^2]\,, \tag{2.14}$$

where A is the amplitude of the eigenfunction. Requiring the norm of each ansatz to be unity, gives

$$A^{(sawtooth)} = \sqrt{\frac{3}{\ell}} \qquad A^{(parabolic)} = \sqrt{\frac{15}{8\ell}} \tag{2.15}$$

Diagrams of both ansatzes are shown in Fig. 2.1.

As outlined in Section 2.2, once we have the ansatz, we then evaluate the action for that ansatz. However for eigenvalue problems, it is standard to set up the variational problem with the "action" being the eigenvalue [3, 24]. Taking this approach, we then vary the eigenvalue, ν, where:

$$\nu = \frac{\int_0^\ell \left(\frac{du}{dx}\right)^2 dx}{\int_0^\ell u^2 dx}\,. \tag{2.16}$$

It is trivial to verify that varying u and requiring the action to be an extremum then gives us (2.11). Inserting (2.13) and (2.14) into (2.16) respectively, we obtain

$$\nu_0^{(sawtooth)} = \frac{12}{\ell^2} = 1.216...\pi^2/\ell^2\,, \tag{2.17}$$

$$\nu_0^{(parabolic)} = \frac{10}{\ell^2} = 1.013...\pi^2/\ell^2\,. \tag{2.18}$$

In this case, our only parameter was the amplitude which was set by the normalization condition. Furthermore, since (2.11) is linear, the amplitude drops out anyway and the

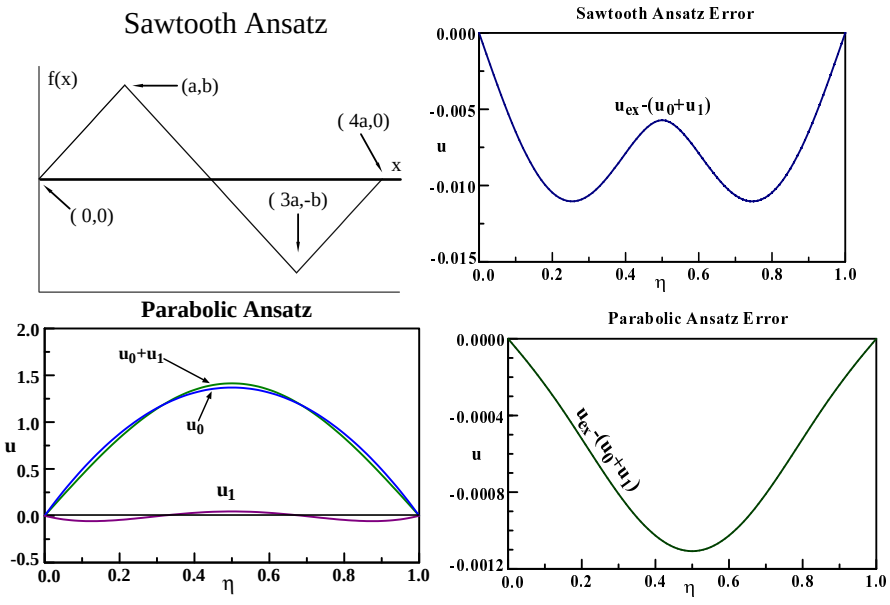

Figure 2.1: plots of the difference between the exact solution and the sum of variational ansatz and the first order correction.

action has only a fixed value and no further variation can be done. Thus the VA for the eigenvalue for each case takes on the value shown above. As far as accuracy is concerned, we see that the sawtooth ansatz is less accurate, with the eigenvalue being only within 22% of the exact value. On the other hand, the parabolic approximation is much better, giving an eigenvalue within 1.3% of the correct value. However, we know this only because we are comparing with the exact solution. Let us now see how we can quantify these accuracies without knowing the correct answer.

2.3.2 The Correction

In the case of the first-order correction to an eigenvalue problem, there will also be an eigenvalue shift as well as a shift in the function. Instead of rederiving our result for eigenvalue

problems, we may simply recognize that this is so, recognize that a shift is needed, and then go directly to (2.9) and (2.10), obtaining:

$$\int_{\mathcal{D}} \left(\frac{\delta^2 L}{\delta u(x) \delta u(x')} \right)_0 u_1(x') dx' + R(x) + 2\delta\nu \, u_0(x) = 0 \,, \tag{2.19}$$

where we have taken $\delta\nu$ to be the shift in the eigenvalue and defined

$$R(x) = \frac{d^2 u_0}{dx^2} + \nu_0 \, u_0 \,. \tag{2.20}$$

Since $\nu_0 = k^2$, then in general

$$\nu = k^2 + \delta\nu \,, \tag{2.21}$$

in which case, from (2.12), (2.19) becomes

$$\frac{d^2 u_1}{dx^2} + k^2 \; u_1 = U(x) \,, \tag{2.22}$$

where

$$U(x) = -R(x) - 2\delta\nu \, u_0(x) \,. \tag{2.23}$$

Eq. (2.19) is a linear problem, even when the analogy of (2.11) is nonlinear. Whence we can always solve it with linear techniques, and in this case, the solution of (2.22) is:

$$u_1 = -iC_+ e^{ikx} - iC_- e^{-ikx} + \int_0^x U(x') \frac{\sin(k(x - x'))}{k} dx' \tag{2.24}$$

where $C_\pm$ are the two constants of integration. As one may verify by integrating by parts,

$$\int_0^x U(x') \frac{\sin(k(x - x'))}{k} dx' \; = \; \frac{du_0}{dx}(0) \, \frac{\sin(kx)}{k} \; - \; u_0(x) \; - \; \frac{\delta\nu}{k} \int_0^x \; u_0(x') \, \sin(k(x - x')) \, dx' \,. \tag{2.25}$$

Now we impose our boundary conditions and the normalization condition. At the left end, $u(0) = 0$ gives $C_+ = -C_-$. At the right end, $u(\ell) = 0$ gives

$$C_+ = -C_- = -\frac{1}{2k}\,\frac{du_0}{dx}(0) + \frac{\delta\nu}{2k\sin(k\ell)}\int_0^\ell u_0(x')\,\sin(k(\ell - x'))\,dx'\,. \tag{2.26}$$

Imposing the condition that the norm be unity to order ϵ will give

$$\int_0^\ell u_0(x')\,u_1(x')\,dx' = 0\,, \tag{2.27}$$

which along with (2.26) will give us the value for $\delta\nu$.

Let us now consider our two ansatzes. With the above, it is straight forward to evaluate the integrals analytically as well as numerically. We will not give the analytical expressions due to their complexity. The numerical values are

$$C_+^{(sawtooth)} = 0.0873...A\,, \quad \text{and} \quad \delta\nu^{(sawtooth)} = -0.219...\pi^2/\ell^2\,, \tag{2.28}$$

$$C_+^{(parabolic)} = -0.119...A\,, \quad \text{and} \quad \delta\nu^{(parabolic)} = -0.013...\pi^2/\ell^2\,, \tag{2.29}$$

whereby we note that the corrections to the eigenvalues are indeed essentially what we had estimated from our knowledge of the exact solution. Thus $\delta\nu$ does indeed give a quantitative estimate of the accuracy of these two VA's. As we had pointed out earlier, the parabolic ansatz is more accurate than the sawtooth, and the above numbers gives a quantitative justification of that statement.

Naturally, the corrected eigenvalues will be more accurate, and these values are

$$(\nu_0 + \delta\nu)^{(sawtooth)} = 0.99675...\pi^2/\ell^2\,, \quad (\nu_0 + \delta\nu)^{(parabolic)} = 0.99998...\pi^2/\ell^2\,, \tag{2.30}$$

which gives an almost five 9's agreement for the corrected parabolic approximation.

The correction to an eigenvalue is just one possible quantitative estimate of VA accuracy. Another quantitative estimate is the rms error of the ansatz. Taking the above expressions for (2.24) and defining the relative rms error, E_{rms}, by

$$E_{rms}^2 == \frac{\int_0^\ell (u_1)^2 dx}{\int_0^\ell (u_0)^2 dx}\,, \tag{2.31}$$

we find that for each of our approximations,

$$E_{rms}^{(sawtooth)} = 0.124...\,, \quad E_{rms}^{(parabolic)} = 0.038...\,. \tag{2.32}$$

Obviously again the parabolic ansatz is the most accurate.

2.4 The Korteweg Devries Equation

This equation is a well known nonlinear equation [9] and we will use it to demonstrate how one can obtain estimates of the error of a VA in a nonlinear system. We shall apply this method to finding soliton (localized traveling wave) solutions of the Korteweg - de Vires (KdV) equation, which is

$$u_t + 6uu_x + u_{xxx} = 0\,. \tag{2.33}$$

Soliton solutions of the form $u(x,t) = U(\xi)$ where $\xi = x - ct$, exist where c is the wavespeed. The amplitude of such a wave, U, then satisfies the ODE

$$-cU_\xi + 6U_\xi U + U_{\xi\xi\xi} = 0\,. \tag{2.34}$$

Since these soliton solutions vanish as $\xi \to \pm\infty$, we may integrate this equation once to obtain the equation

$$-cU + 3U^2 + U_{\xi\xi} = 0\,. \tag{2.35}$$

From (2.35) one may construct the Lagrangian

$$L = -\frac{1}{2}cU^2 + U^3 - \frac{1}{2}(U_\xi)^2 \,. \tag{2.36}$$

Let us take a gaussian ansatz of the form:

$$U_0(\xi) = A\exp(-\xi^2/\rho^2) \,. \tag{2.37}$$

where U_0 has two parameters; an amplitude A and a width ρ. Given this ansatz, we may construct the action, S:

$$S = \int_{-\infty}^{+\infty} L[u_0(\xi)]d\xi = -\frac{\sqrt{2\pi}}{4}\left(cA^2\rho - \frac{4}{\sqrt{6}}A^3\rho + \frac{A^2}{\rho}\right) . \tag{2.38}$$

Note that in this case, c is a control parameter and is not to be varied. Varying the action with respect to the trial function parameters will result in two Euler-Lagrange equations whose solution(s) will give "the closest fit" to the exact solution. These equations reduce to

$$\frac{\delta S}{\delta A} = 0 = c\rho^2 - \sqrt{6}A\rho^2 + 1 \,, \tag{2.39}$$

$$\frac{\delta S}{\delta \rho} = 0 = c\rho^2 - \frac{4}{\sqrt{6}}A\rho^2 - 1 \,, \tag{2.40}$$

whose solutions are

$$A = \frac{\sqrt{6}}{5}c \,, \qquad \rho^2 = \frac{5}{c} \,. \tag{2.41}$$

2.4.1 First Order Correction

We shall now calculate the first order correction to the variational ansatz. As before, we take an expansion as in (2.5),

$$U_e = U_0(\xi; q) \, + \, \epsilon U_1(\xi) \, + \, \ldots \,, \tag{2.42}$$

and insert it into (2.35). In the above, ϵ is a small ordering parameter, $U_0(\xi)$ is the variational ansatz and $U_1(\xi)$ is the first-order correction. Again we note that if (4.12), together with (2.41), is an reasonably accurate approximation, then we would expect the quantity

$$\epsilon R(\xi) = -cU_0 + \frac{1}{2}U_0^2 + U_{0,\xi\xi}\,, \tag{2.43}$$

to be quite small. This then should generate a reasonably small U_1 which would be determined by the linear problem

$$-cU_1 + U_0U_1 + U_{1,\xi\xi} = -R(\xi)\,. \tag{2.44}$$

The problem of solving (2.44) can be simplified if we scale our coordinates and amplitudes. Let us define a new coordinate, y, and new amplitudes, H_0 and H_1, where

$$\xi = \rho y\,, \quad H_0(y) = c\,U_0(\xi)\,, \quad H_1(y) = c\,U_1(\xi)\,, \tag{2.45}$$

in which case (2.43) and (2.44) become

$$\frac{d^2H_1}{dy^2} + (6\sqrt{6}e^{-y^2} - 5)\,H_1 = -R'(y)\,, \tag{2.46}$$

where

$$R' = \frac{\sqrt{6}}{5}e^{-y^2}\left[(4y^2 - 7) + 3\sqrt{6}e^{-y^2}\right]. \tag{2.47}$$

The boundary conditions on H_1 are that $H_1 \to 0$ as $y \to \pm\infty$. There will be two homogeneous solutions of (2.47) and one particular solution. The two homogeneous solutions approach a linear combination of $\exp(\pm\sqrt{5}y)$ as $y \to \pm\infty$. The boundary conditions will give a unique solution for H_1, provided that neither homogeneous solution is a bound state (which is the case).

To see this, we start integrating from the left end. We eliminate the homogeneous solution that approaches $\exp(-\sqrt{5}y)$ as $y \to -\infty$, leaving us with the particular solution and one homogeneous solution, H_{1h} which will in general approach $\exp(\sqrt{5}y)$ as $y \to -\infty$. We take the particular solution, H_{1p}, to also vanish as $y \to -\infty$. Then we integrate H_{1h} and H_{1p} from $y = -\infty$ to $y = \infty$. Each solution will in general contain the component $\exp(\sqrt{5}y)$ as $y \to \infty$. We now construct a linear combination $H_1 = H_{1p} + \gamma H_{1p}$ and then determine γ such that the exponentially increasing component of H_1 vanishes as $y \to \infty$, resulting in a unique, bounded solution, shown in Fig. 2.

In Fig. 3, we show the ansatz H_0 compared to the sum $H_0 + H_1$. As one can see, the first-order correction mainly corrects for the more rapid decay of the gaussian at large y. In Fig. 4, we show the difference between the exact solution, H_e, and $H_0 + H_1$, which will indicate what the second-order correction would be. Here we note that the largest remaining correction is in the central region of the pulse. [Since the KdV equation is nonlinear, after the first-order correction we would have a nonzero second-order correction, which would therefore be largest wherever the amplitude was largest. Here we see that this is indeed the case.]

As already mentioned, there are several ways in which one could quantitatively measure the accuracy of an ansatz, depending on what quantity one was interested in. We shall consider two possibilities. First, the standard rms error (2.31) can again be calculated. This would be appropriate as a measure of the global error in the pulse shape. Here we find that $E_{rms} = 0.0380...$, which indicates that this is a quite good global approximation. However, if one were interested in calculation soliton-soliton interactions wherein the overlap of the tails

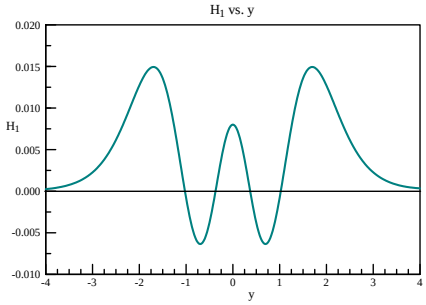

Figure 2.2: the first-order correction, $H_1(y)$, to the gaussian ansatz.

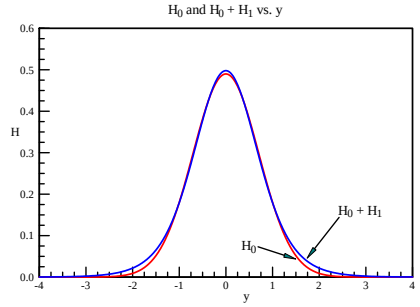

Figure 2.3: $H_0(y)$ and $H_0(y) + H_1(y)$.

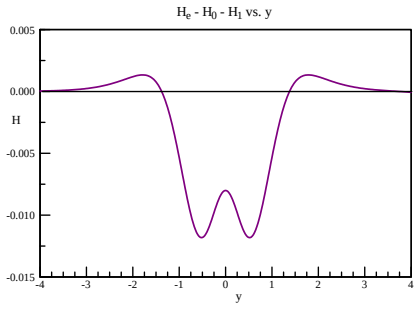

Figure 2.4: the exact solution, $H_e(y)$, minus the sum of the ansatz and the first-order correction, $H_0(y) + H_1(y)$.

were important, then the situation could become different. So the quantitative measure of a VA may well depend on what application it was destined to be applied to.

Let us now be definite, and calculate a quantitative measure for this case. For the gaussian approximation, we have from Fig. 3 that the width at half-height is $w_{1/2} = 1.594....$ If one were to plot the tail amplitude vs. this width, as in Fig. 6, one readily would see that the gaussian ansatz is an inferior approximation for the tails. For example, if one chose to have the solitons separated such that the tail amplitude in the region of the next soliton would be no more than 0.001, the dashed line in Fig. 6 shows that a soliton-soliton separation of only 1.56 widths would be sufficient. However if we add the first-order correction to the ansatz, $H_0 + H_1$, which is also shown in Fig. 6, then we would come to a different conclusion. The curve $H_0 + H_1$ shows that the ansatz plus correction, at a width of 1.56, would have an amplitude of ≈ 0.008, which is eight times too large. Looking at where the separation should actually be, we see that the tails of $H_0 + H_1$ do not decay to 0.001 until at least 2.1 widths. Thus since the ratio of these widths is $2.1/1.59 = 1.32$, a measure of the VA accuracy in this case would be $\pm 32\%$, considerably more than the 3.8% indicated by the rms error.

2.5 Conclusion

In this paper we have established a method for quantifying a measure of the accuracy of variational approximations, and these quantitative estimates can be obtained without the use of exact solutions. The only further calculation required beyond the calculation of the variational solution, is the solution of a nonhomogeneous linear equation.

We have also pointed out that the quantitative measure of any variational approximation

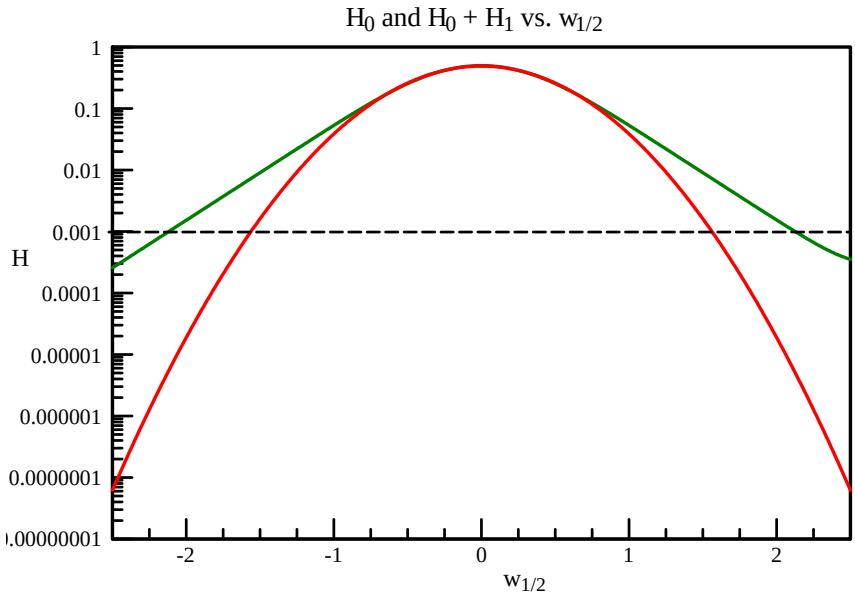

Figure 2.5: A log(H) plot showing the amplitudes of the tails vs. the width at half-height, with H_0 being the lower curve and with $H_0(y) + H_1(y)$ being the upper curve. The dashed line is an example - see the text.

needs to be based on the intended use of the solution. Depending on the use, the VA could either be quite acceptable or could even be unacceptable. The smallness of the correction, or the smallness of its deviation from some important property of the exact solution, should be the quantitative measure of the validity of any VA.

This work also opens up further future approaches to the modeling of physical and mathematical systems. It is now possible for one to chose an acceptable analytical model close to a system being studied, obtain a VA for that system, and then use the method outlined here to estimate how accurate any obtained results were, by estimating the error from the first-order correction. Furthermore, by using the first-order correction found, one may then improve on the predictions of that VA.

LOCATING EMBEDDED SOLITONS IN A CHI(2):CHI(3) SYSTEM USING A VARIATIONAL APPROXIMATION

3.1 Embedded Solitons

A localized ordinary soliton usually has a propagation constant that does not fall into the continuous spectrum of radiation modes. Consider the case of the NLS equation given by

$$i\frac{\partial u}{\partial z} + \frac{1}{2}\frac{\partial^2 u}{\partial x^2} + \frac{\gamma}{4}|u|^2 u = 0 \tag{3.1}$$

To find the soliton solution admitted by (3.1) consider a search for stationary state solutions (i.e., an eigenstate of the Hamiltonian which allows for the z-dependence to be factored out) by taking:

$$u(x,z) = e^{ikz}U(x) \tag{3.2}$$

Substituting (3.2) into (3.1) (and dividing off a factor of e^{ikz}) yields an equation for the propagation of the field envelope

$$U''(x) - 2kU(x) + \frac{\gamma}{2}U^3(x) = 0 \tag{3.3}$$

The linear dispersion relation will determine for which values of the propagation constant, k, there will be localized structure (i.e. exponential behavior), versus pure radiation modes. If $k > 0$, the solution will be localized. If $k < 0$, integration of the NLS equation exhibits pure radiation modes. The localized soliton solution is found to be

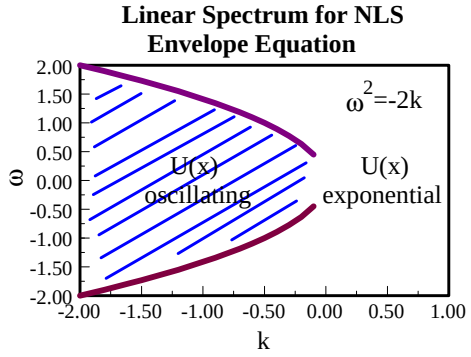

Figure 3.1: linear dispersion relation for NLS envelope equation

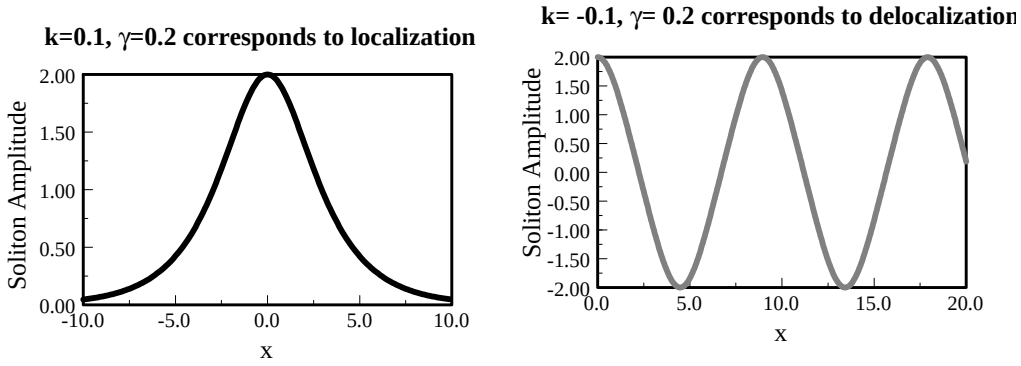

Figure 3.2: numerical integration of NLS equation; $k < 0$ (pictured on the right) yields oscillations while $k > 0$ (pictured on the left) yields localization

$$U(x) = 2\sqrt{\frac{2k}{\gamma}}sech(\sqrt{2k}x) \tag{3.4}$$

Consider a similar (hypothetical) dispersion relation for a two component system as shown in Figure 3.3. The dispersion relation for this system has a multiple branch structure. More specifically, there are regions of ω in which one branch corresponds to k real, while the other branch corresponds to k imaginary. Within these partial gaps in the dispersion

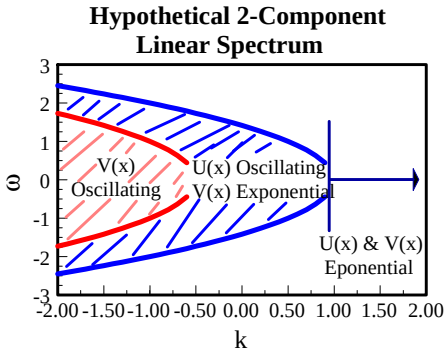

Figure 3.3: multi-component linear dispersion relation

relation, there exist quasi-solitary waves with non vanishing oscillatory tails. It has been observed that (under the appropriate circumstances) there may exist discrete values of ω for which the amplitude of the tail vanishes. This would represent a localized object at a discrete value of ω for which a real value of $k = k_{ES}$ exists. This value of ω lies within the continuous part of the wave number spectrum (which does not support the existence of pure solitons). For this reason, these solutions are referred to as embedded solitons (ES). A more analytic justification of the existence of such a soliton solution is given in [6].

3.2 Type II, CHI(2):CHI(3) System

3.2.1 The Model

Soliton solutions in a three wave (3W) system have been detailed in [7]. The system combines two orthogonally polarized fundamental frequency (FF) components and a single second harmonic (SH) component. The governing system incorporates birefringence and both $\chi^{(2)}$ and $\chi^{(3)}$ nonlinearities. Such a system has physical significance for solitons in optical systems

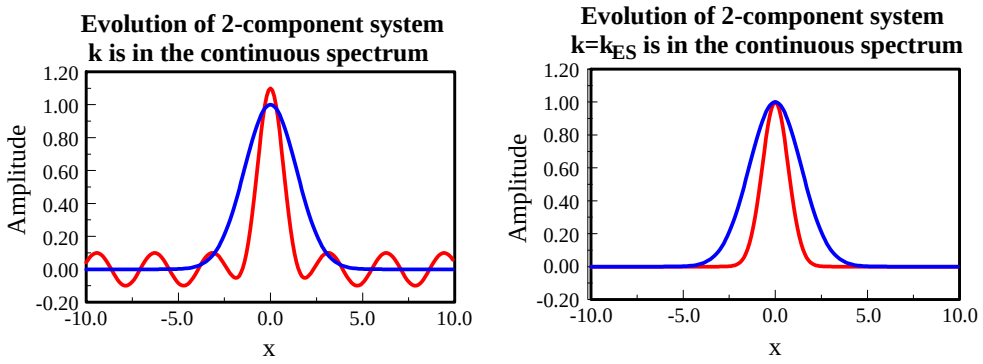

Figure 3.4: two component evolution: k in continuous spectrum; slide 1: one component localized, the other delocalized, slide 2: both components localized

in which the material birefringence is employed to phase-match two orthogonal linearly polarized components of the FF wave to a single SH component. This is known as a type-II $\chi^{(2)}$ interaction. In the presence of a uniform media which admits the phase-matched $\chi^{(2)}$ interaction, the Kerr nonlinearity is typically weaker than its quadratic counterpart. As discussed in [2], within certain optical crystals the $\chi^{(2)}$ and $\chi^{(3)}$ nonlinearities can be made comparable. This is accomplished by aligning the beam's Poynting vector relative to the crystallographic axis.

Suppose u and v are the complex envelopes of the two components of the FF field, and w is the single SH component. The complete evolution equations for the 3W system (taking into account the $\chi^{(2)}$:$\chi^{(3)}$ interaction, self-phase modulation (SPM), cross-phase modulation (CPM), and four-wave mixing (FWM)) are:

$$\imath u_z + \frac{1}{2}u_{xx} + v^* w + \gamma_1 \left(\frac{1}{4}|u|^2 + \frac{1}{6}|v|^2 + 2|w|^2 \right) u + \frac{1}{12}\gamma_1 v^2 u^* + \gamma_2 |w|^2 v + bu = 0 \quad (3.5)$$

$$\imath v_z + \frac{1}{2}v_{xx} + u^* w + \gamma_1 \left(\frac{1}{4}|u|^2 + \frac{1}{6}|v|^2 + 2|w|^2 \right) v + \frac{1}{12}\gamma_1 u^2 v^* + \gamma_2 |w|^2 u - bv = 0 \quad (3.6)$$

$$2\imath w_z + \frac{1}{2}w_{xx} + uv - qw + 2\gamma_1 \left(|u|^2 + |v|^2 + 2|w|^2 \right) w + \gamma_2 \left(uv^* + u^* v \right) w = 0 \quad (3.7)$$

In the above system, b is the birefringence coefficient, and q is the phase-mismatch parameter that controls the second harmonic generation process. The $\chi^{(2)}$ coefficient has been normalized to unity, while γ_1 and γ_2 are the two $\chi^{(3)}$ coefficients. All of the above stated constants are real. The only constraint is that γ_1 and γ_2 are of the same sign. $\gamma_{1,2} > 0$ corresponds to self-focusing while $\gamma_{1,2} < 0$ corresponds to a self-defocusing nonlinearity.

3.2.2 The Linear Dispersion Relation

Consider the stationary soliton solutions of the form

$$u(z,x) = e^{\imath kz} U(x), \quad v(z,x) = e^{\imath kz} V(x), \quad w(z,x) = e^{2\imath kz} W(x)$$

Upon substituting these forms into the governing equations, a system of ODE's is obtained. This system is determined by:

$$\begin{aligned}
-(k-b)U &+ \frac{1}{2}U'' + VW + \gamma(\frac{1}{4}U^2 + \frac{1}{4}V^2 + 2W^2)U + \frac{1}{6}\gamma W^2 V = 0 \quad (3.8)\\
-(k+b)V &+ \frac{1}{2}V'' + UW + \gamma(\frac{1}{4}U^2 + \frac{1}{4}V^2 + 2W^2)V + \frac{1}{6}\gamma W^2 U = 0\\
-(4k+q)W &+ \frac{1}{2}W'' + UV + 2\gamma(U^2 + V^2 + 2W^2)W + \frac{1}{3}\gamma UVW = 0
\end{aligned}$$

It has been assumed that $\gamma_2 = \gamma_1/6 = \gamma$. This assumption is discussed in [7]. The above equations can be decoupled by taking

$$V = W = 0 \quad or \quad U = W = 0 \quad or \quad U = V = 0 \tag{3.9}$$

giving rise to

$$-(k-b)U + \frac{1}{2}U'' + \frac{\gamma}{4}U^3 = 0 \tag{3.10}$$

$$-(k+b)V + \frac{1}{2}V'' + \frac{\gamma}{4}V^3 = 0$$

$$-(4k+q)W + \frac{1}{2}W'' + 4\gamma W^3 = 0$$

There exist exact soliton solutions to these equations:

$$U = 2\sqrt{\frac{2(k-b)}{\gamma}}sech\left(\sqrt{2(k-b)}x\right) \tag{3.11}$$

$$V = 2\sqrt{\frac{2(k+b)}{\gamma}}sech\left(\sqrt{2(k+b)}x\right)$$

$$W = \sqrt{\frac{4k+q}{2\gamma}}sech\left(\sqrt{2(4k+q)}x\right)$$

To determine the regions of k which may allow for the formation of an ES, we must first consider the linear dispersion relation for the governing system (3.5)-(3.7). The linear dispersion relation is determined by

$$\omega_u^2 = 2(k-b) \qquad \omega_v^2 = -2(b+k) \qquad \omega_w^2 = -2(q+4k) \tag{3.12}$$

In order for each respective component to be localized, it must be the case that

$$u_{comp} : k > b \quad v_{comp} : k > -b \quad w_{comp} : k > -\frac{q}{4} \tag{3.13}$$

For the purpose of this work, it will be assumed that either birefringence is set ($b = 1$) or it is neglected ($b = 0$). We seek a component arrangement with respect to the linear spectrum in which two of the components are localized, while the third component has oscillatory behavior away from the core. The core of the third component should be soliton-like and the oscillations should be relatively small. With the birefringence set, there are not many arrangements that fit these requirements. Observe that the v-component has no opportunity to be an ES. There is no arrangement for which the u and w components can simultaneously be localized while v contains a small oscillating tail.

There exist two possible varieties of ES in equations (3.5)-(3.7). The first possibility is that the ES exists within the u-component. In fact, this is the only possible scenario for an ES in this system if the birefringence is considered. The other possibility for the existence of an ES occurs only when the birefringence can be neglected. In this case, both the u and v-components are localized (with the same linear dispersion relation) for $k > 0$. In this situation there exists a small q-dependent neighborhood to the right of zero which may support the existence of an ES on the SH component. This neighborhood exists for

$$k \in \left(0, -\frac{q}{4}\right) \quad where \;\; q < 0 \tag{3.14}$$

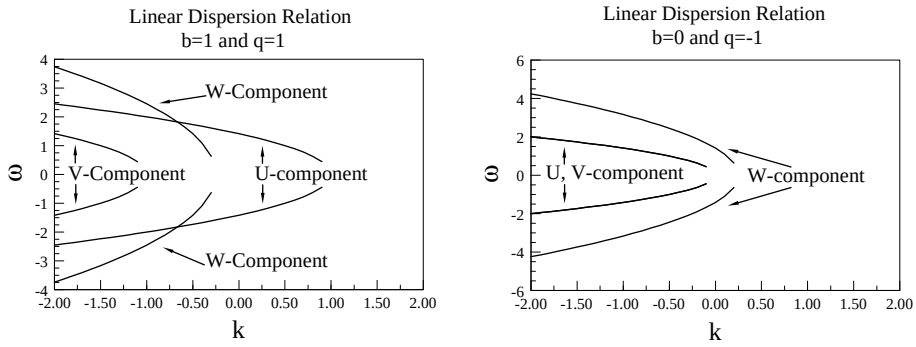

Figure 3.5: linear dispersion relation for the $\chi^{(2)} : \chi^{(3)}$, type II system

3.2.3 The Variational Approximation

The Lagrangian density from which the governing equations can be derived is given by

$$\begin{aligned} L &= \frac{1}{2}(\imath u^*\partial_z u + \imath v^*\partial_z v + 2\imath w^*\partial_z w + c.c.) + \frac{1}{2}\left(\left|\frac{du}{dx}\right|^2 + \left|\frac{dv}{dx}\right|^2 + \left|\frac{dw}{dx}\right|^2\right) \\ &+ b(|u|^2 - |v|^2) - q|w|^2 + (u^*v^*w + w^*uv) + \frac{\gamma_1}{8}(|u|^4 + |v|^4) + 2\gamma_1(|u|^2 + |v|^2 + |w|^2)|w|^2 \\ &+ \gamma_2(|u|^2|v|^2 + u^*v|w|^2 + v^*u|w|^2) + \frac{\gamma_1}{24}\left[(u^*v)^2 + (v^*u)^2\right] \end{aligned} \tag{3.15}$$

where c.c. is the associated complex conjugate.

The method employed in this paper for establishing a criteria for embedded solitons is outlined in [18]. Up until the appearance of this work, locating ESs has primarily been accomplished numerically in a "hit or miss" fashion. The authors of the above cited work use a variational approximation (VA) to develop a criteria for finding ES's in a second harmonic generation model. The approach supposes that for wave numbers close to k_{ES}, (those wave

numbers close to a wave number for which an embedded soliton exists), there exists a family of delocalized solitons with small amplitude oscillating tails in the ES component that vanish at $k = k_{ES}$. The tail of such a delocalized structure (taking into account the phase shift) will be assumed to take the form

$$V_{tail} = a_{u,v,w} \cos(\kappa_{u,v,w} x) e^{\imath \alpha_{u,v,w}(z)} \tag{3.16}$$

The core soliton form is taken to be a Gaussian for the trial function. The tail behavior of the delocalized component will be taken into consideration with the addition of the above tail ansatz into the variational ansatz. In addition, it will be assumed that all three components will have identical core widths. This assumption does not pose a major restriction on the VA method. The only region in which this assumption breaks down is when k is near the boundary of the continuous spectrum [7]. The core ansatz for all three components is taken to be:

$$V_{sol} = A_{u,v,w} \exp\left[-(x^2/\rho^2) + \imath \alpha_{u,v,w}\right] \tag{3.17}$$

where $A_{u,v,w}$ are the real amplitudes, ρ the common width, and $\alpha_{u,v,w}$ the phase at the center of the respective soliton component. With the tail added to the necessary component, the full variational ansatz is

$$V_{v,w}(x) = V_{sol} \quad and \quad V_u(x) = V_{sol}(x) + V_{tail}(x) \tag{3.18}$$

The three variational solution forms are substituted back into the Lagrangian density given in (3.15). From this, it is necessary to calculate the effective Lagrangian.

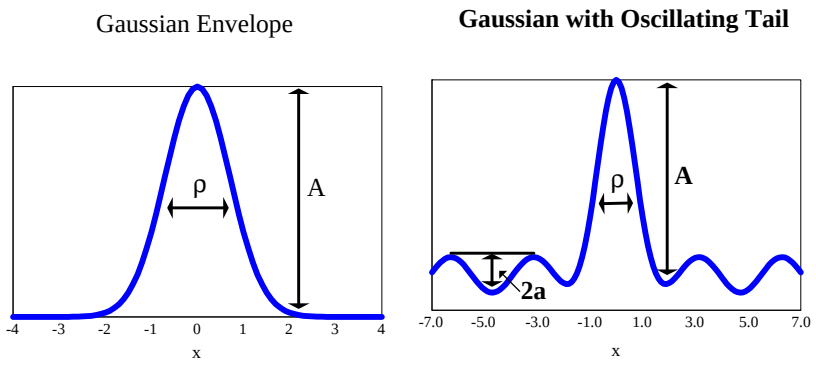

Figure 3.6: variational ansatz for the $\chi^{(2)} : \chi^{(3)}$, type II system

$$L_{eff} = \int_{-\infty}^{\infty} L_{density} dx \tag{3.19}$$

The difficulty is that, in general, L_{eff} does not exist. It contains terms that will converge, as well as terms that will not. More specifically, the terms in $L_{density}$ which cause this difficulty are given in expression (3.20).

$$\begin{aligned} \frac{3}{8}\gamma a^2 \quad &+ \quad \frac{1}{2}\gamma a^2 \cos(2\kappa x) + \frac{1}{8}\gamma a^2 \cos(4\kappa x) + 2\kappa^2 - 2\kappa^2 \cos(2\kappa x) + 4b \\ &+ \quad 4b\cos(2\kappa x) - 4(\frac{\partial}{\partial z}\alpha(z)) - 4(\frac{\partial}{\partial z}\alpha(z))\cos(2\kappa x) \end{aligned} \tag{3.20}$$

This can be remedied by utilizing the phase, κ, in the ansatz of the oscillating tail of the delocalized component. It is possible to solve for κ in a such a way as to keep L_{eff} finite. The terms which are pure radiation will average out, leaving a necessity to balance the remaining terms. The phase which accomplishes this balance, κ, has been calculated to be (depending on which component is delocalized)

$$\begin{aligned} \kappa_u^2 &= -\frac{3}{16}\gamma_1 a_u^2 - 2b + 2\frac{d}{dz}\alpha_u(z) \\ \kappa_w^2 &= -3\gamma_1 a_w^2 + 2q + 4\frac{d}{dz}\alpha_w(z) \end{aligned} \tag{3.21}$$

The equations for the evolution of the parameters in the ansatz can now be established via L_{eff}. Varying the effective Lagrangian with respect to each of the parameters will produce an Euler-Lagrange equation. In the case of the exact solution this functional derivative should be zero. Of course the ansatz solution form is approximate, and hence it will result in a set of Euler-Lagrange equations ≈ 0. Four evolution equations can be obtained according to:

$$\frac{\partial L_{eff}}{\partial A_{u,v,w}} = \frac{\partial L_{eff}}{\partial \rho} = 0 \tag{3.22}$$

Note that since the ansatz parameters are static, the functional derivative reduces to a partial derivative. The four associated Euler-Lagrange equations for the evolution of the static parameters are (respectively):

$$\left[\frac{1}{\rho^2} + 2(k-b)\right]\frac{A_u}{\sqrt{2}} - \frac{2}{\sqrt{3}}A_v A_w - \frac{\gamma}{4}A_u(A_u^2 + A_v^2) - 2\gamma\left[A_u + \frac{A_v}{12}\right]A_w^2 = 0 \tag{3.23}$$

$$\left[\frac{1}{\rho^2} + 2(k+b)\right]\frac{A_v}{\sqrt{2}} - \frac{2}{\sqrt{3}}A_u A_w - \frac{\gamma}{4}A_v(A_u^2 + A_v^2) - 2\gamma\left[A_v + \frac{A_u}{12}\right]A_w^2 = 0 \tag{3.24}$$

$$\left[\frac{1}{\rho^2} + 8k + 2q\right]\frac{A_w}{\sqrt{2}} - \frac{2}{\sqrt{3}}A_u A_v - 4\gamma A_w^3 - 2\gamma\left[A_u^2 + \frac{1}{6}A_u A_v + A_v^2\right]A_w^2 = 0 \tag{3.25}$$

$$\left[b - k + \frac{1}{2\rho^2}\right]\frac{A_u^2}{\sqrt{2}} + \left[-b - k + \frac{1}{2\rho^2}\right]\frac{A_v^2}{\sqrt{2}} + \left[-q - 4k + \frac{1}{2\rho^2}\right]\frac{A_w^2}{\sqrt{2}} + \frac{2}{\sqrt{3}}A_u A_v A_w + \frac{\gamma}{16}(A_u^2 + A_v^2)^2 + \gamma\left[A_u^2 + \frac{1}{6}A_u A_v + A_v^2\right]A_w^2 = 0 \tag{3.26}$$

The small amplitude of the oscillating tail is an extra variational degree of freedom. This will give rise to the existence of another Euler-Lagrange equation. It is obtained by

$$\frac{\partial L_{eff}}{\partial a_{u,v,w}}|_{a=0} = 0 \tag{3.27}$$

We are interested in the "location" (in parameter space) of the ES, which by itself has no tail (a=0). *After* taking the above functional (partial) derivative, a is taken to be zero. This means that, prior to varying in a, only terms in L_{eff} which are linear in a will be kept. The fifth Euler-Lagrange equation depends on which of the components has the small oscillatory tail. These two variational equations have been determined for u and w respectively:

$$U_{comp} \quad : \tag{3.28}$$

$$6\sqrt{3}\gamma A_u^3 \quad + \quad 48\sqrt{3}\gamma A_u A_w^2 + 6\sqrt{3}\gamma A_v^2 A_u + 4\sqrt{3}\gamma A_v A_w^2 + 36\sqrt{2}A_v A_w e^{\frac{1}{12}(b-k)\rho^2} = 0$$

$$W_{comp} \quad : \tag{3.29}$$

$$8\sqrt{3}\gamma A_u A_v A_w \quad + \quad 48\sqrt{3}\gamma A_w(A_u^2 + A_v^2) + 96\sqrt{3}\gamma A_w^3 + 36\sqrt{2}A_u A_v e^{-(\frac{1}{12}q+\frac{1}{6}k)\rho^2} = 0$$

An assumption has been made on the two Kerr coefficients, γ_1 and γ_2. They have been set so as not to be independent. If the cubic nonlinearity is induced by the response of the dielectric medium [7], then it is the case that

$$\gamma_2 = \gamma_1/6 \tag{3.30}$$

In equations (3.28) and (3.29), $\gamma = \gamma_1$. In addition, stationary state solutions will be saught. This allows the z-dependence to be factored using using (3.31).

$$\frac{d}{dz}\alpha_u(z) = \frac{d}{dz}\alpha_v(z) = \frac{1}{2}\frac{d}{dz}\alpha_w(z) = k \tag{3.31}$$

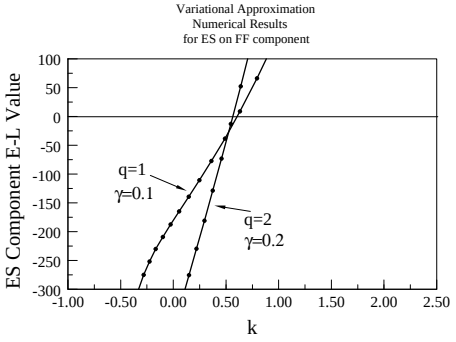

Figure 3.7: variational predictions for the k-value of embedded solitons for $b = 1$

The above Euler-Lagrange equations are then solved numerically to recover an initial estimate for the three core amplitudes $A_{u,v,w}$, a value for the component width ρ, and an approximate wave number, k, for which the ES exists. This was done by choosing a control parameter (in this case the amplitude of the core of the w-component), and using it to simultaneously solve the remaining four equations. The fifth Euler-Lagrange equation (representing the evolution equation obtained by varying the terms in L_{eff} which are linear in a) is monitored for passing through a zero. If this crossing corresponds to a value of k for which the appropriate localized and delocalized structure is present, it is a possible candidate for an embedded soliton. Consider the case in which the small oscillating tail is on the u component. Two possible embedded soliton candidates were located using the variational approximation. The numerical plot revealing the wave numbers is given in figure (3.7). This is a picture of the crossing of the fifth Euler-Lagrange equation versus k.

As discussed earlier, in order for the delocalized structure to be the w-component (with u and v localized), birefringence must be set to zero. In addition, the SH control parameter,

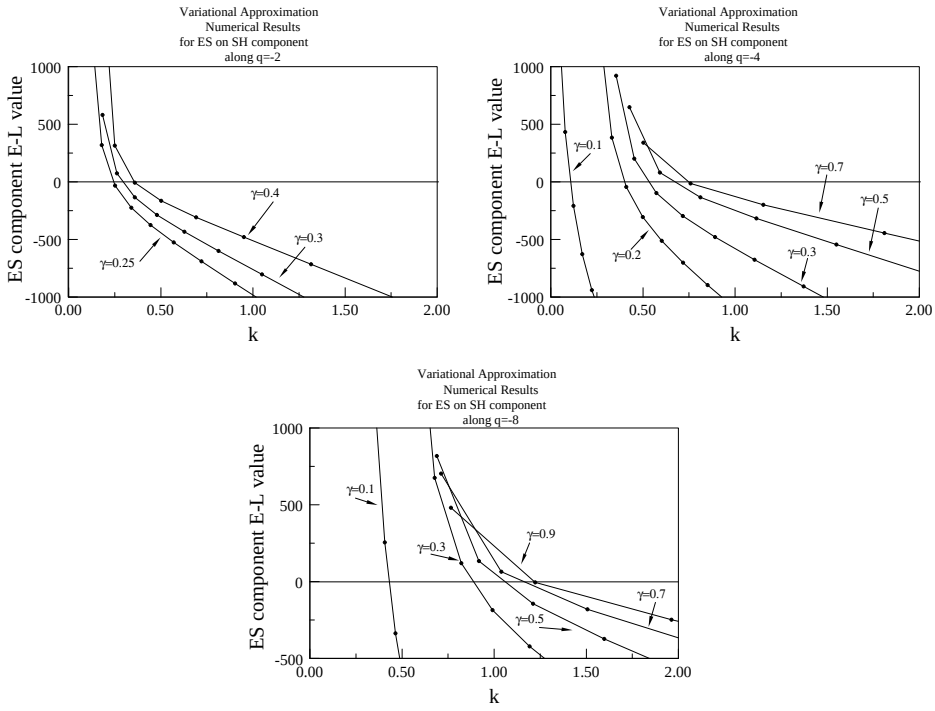

Figure 3.8: variational predictions for the k-value of embedded solitons for $b = 0$

q, must be taken to be a negative number. Embedded solitons were located along $q = -2$, $q = -4$, and $q = -8$. Solving the variational equations using the w-component EL equation, as well as the above mentioned parameter setting, estimates for the location of the ES's were established. The numerical plots for these wave numbers are given in figure (3.8).

3.2.4 Numerical Integration

The variational approximation provides initial data to search for these possible embedded soliton candidates numerically. To accomplish this, the system of ODEs in (3.8) is integrated using an adaptive fourth order Runge-Kutta method. For each ES candidate, the numerical integration was performed repeatedly throughout neighborhoods of $k = k_{ES}$ in an attempt to

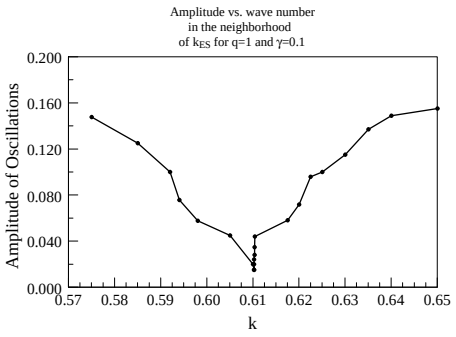

Figure 3.9: plot of oscillating amplitude in a neighborhood of $k = k_{ES} \approx 0.61$

establish a region where an appreciable drop in the oscillatory amplitude could be observed. It is worth mentioning that no value of k_{ES} was located such that the oscillatory tails vanish. The decreasing trend in the amplitude was tracked to six decimal place accuracy for each ES candidate. For the case when $q = 1$ and $\gamma = 0.1$, the VA produced an estimated k_{ES} value at k≈0.62. The result of numerical integration yielded an estimate for k_{ES} much closer to k≈0.61. A numerical plot of the maximum amplitude of the oscillatory component vs. k is given in figure (3.9).

Each of the points in figure (3.9) were obtained "by hand" in the sense that the amplitude was manually extrapolated from each numerical plot of the integration. This is the reason for the "jagged" quality of the curve. Notice also that the amplitude does not cross through a zero. The amplitude is a signed quantity. Figure (3.10) is a snapshot of the numerical integration of the three components in the neighborhood of k_{ES}≈0.610251. At this value of k, the amplitude of the oscillations is about $A \approx 0.01495$. In order to understand what is happening around the value of k where the amplitude starts to fall off rapidly, we need to consider the phase of the oscillation.

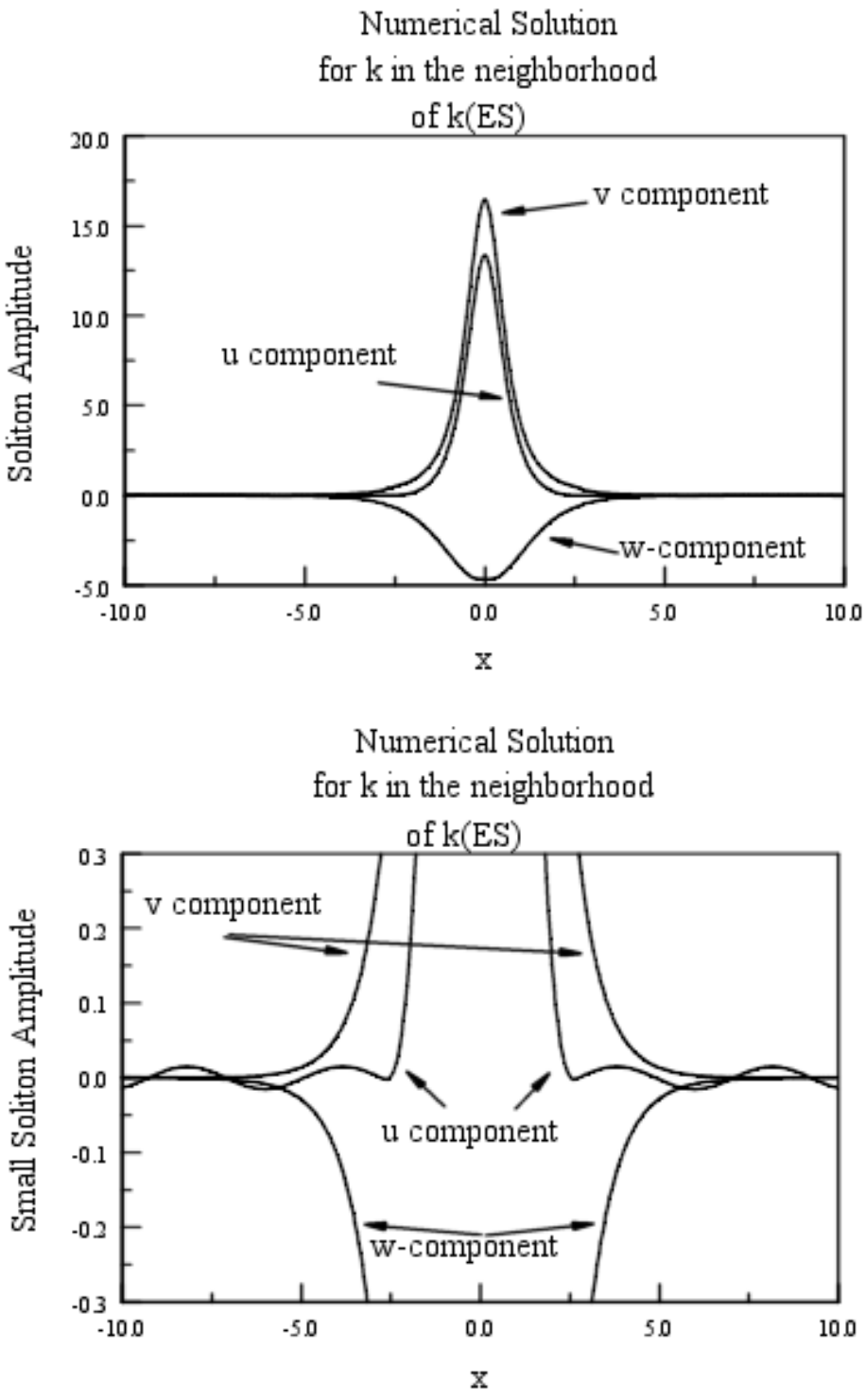

Figure 3.10: numerical integration of $\chi^{(2)} : \chi^{(3)}$, type II system for k_{ES}≈0.610251

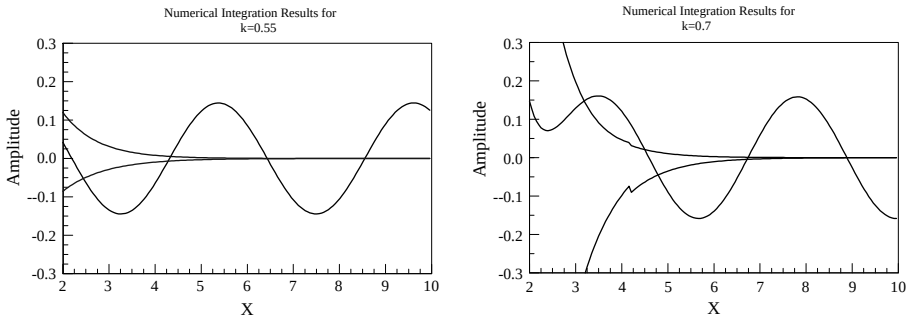

Figure 3.11: π phase shift of asymptotic delocalization in the $\chi^{(2)} : \chi^{(3)}$, type II system

Table 3.1: numerical information for embedded solitons in the fundamental component of the $\chi^{(2)} : \chi^{(3)}$, type II system

q	γ	VA estimate for k	Initial amplitude of u component	Initial amplitude of v component	Initial Amplitude of SH component	Numerical Integration estimate	Measured % drop in amplitude
1	0.1	0.62	12.3	17.3	-3.16	0.610251	99.87%
2	0.2	0.50	3.38	-6.78	1.56	0.500630	99.98%

There were two criteria by which the possible ES candidates were judged. As indicated, one of these criteria was a significant decreasing tendency in the oscillatory amplitude. The second criteria was that the phase of the oscillating tail shifts by π as k crosses k_{ES}. This would be an indication that the small oscillatory amplitude has gone through a zero. For example, in the case $q = 1$ and $\gamma = 0.1$, it was found that the oscillatory phase shifted by about π between $k = 0.55$ and $k = 0.7$. The phase remained relatively unchanged for $k < 0.55$ and $k > 0.7$. This criteria of the phase shifting by π across k_{ES} was used as a determining factor in all of the candidates identified as a possible ES. The following is a summary of the data found for both predicted ES's on the FF component.

Table 3.2: numerical information for embedded solitons in the harmonic component of the $\chi^{(2)} : \chi^{(3)}$, type II system

q	γ	VA estimate for k	Initial amplitude of FF component	Initial Amplitude of SH component	Numerical Integration estimate for k_{ES}	Rel. Error in VA approx.	Measured % drop in amplitude
-2	0.25	0.22	3.05	-0.85	0.203321	7.5%	94.5%
-2	0.3	0.28	2.80	-0.8	0.286320	2.3%	87.3%
-2	0.4	0.31	3.05	-0.6	0.295429	4.7%	77.8%
-4	0.1	0.12	6.01	-1.95	0.114440	4.6%	93.0%
-4	0.2	0.36	4.07	-1.05	0.359665	0.09%	87.0%
-4	0.3	0.53	3.36	-0.75	0.558539	5.3%	94.0%
-4	0.5	0.65	2.77	-0.5	0.623895	4.0%	97.7%
-4	0.7	0.67	2.21	-0.35	0.658127	1.7%	99.1%
-8	0.1	0.39	7.09	-1.85	0.402118	3.1%	98.5%
-8	0.3	0.76	4.04	-0.70	0.726060	4.4%	99.4%
-8	0.5	1.00	3.25	-0.45	0.998447	0.2%	99.6%
-8	0.7	1.10	2.98	-0.35	1.100130	0.01%	99.6%
-8	0.9	1.20	2.36	-0.25	1.182684	1.4%	96.8%

A total of thirteen ES's were identified for the SH component. In each case, both a significant decrease in amplitude and phase shift by approximately π across the wave number k_{ES} was identified. Along each branch of q, the approximate values of k vs. γ for which ES's are predicted to exist are plotted in figure (3.12).

3.3 Embedded Solitons in a CHI(2):CHI(3), Type I System

Consider the $\chi^{(2)} : \chi^{(3)}$, type I system given by

$$\begin{aligned} \imath u_z + \frac{1}{2}u_{xx} + u^* v - (|u|^2 + 2|v|^2)u = 0 \\ \imath v_z + \frac{1}{4}v_{xx} - \beta v + u^2 - 2(2|u|^2 + |v|^2)v = 0 \end{aligned} \tag{3.32}$$

This model is presented in [23]. The above optical system may be derived from the La-

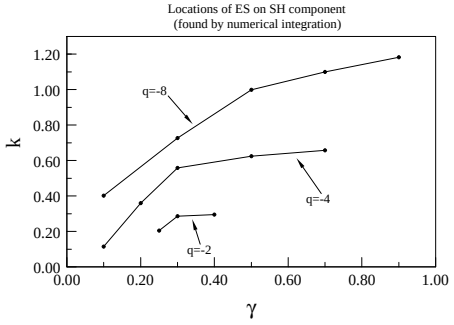

Figure 3.12: locations of embedded solitons in parameter space; obtained by numerical integration

grangian density given by

$$L_{density} = \frac{\imath}{2}(u^* u_z - u_z^* u) + \frac{\imath}{4}(v^* v_z - v_z^* v) - \frac{1}{2}|u_x|^2 - \frac{1}{8}|v_x|^2 - \frac{1}{2}\beta|v|^2 \\ + \frac{1}{2}(u^{*2} v + u^2 v^*) - \frac{1}{2}(|u|^4 + 4|u|^2|v|^2 + |v|^4) \tag{3.33}$$

The stationary state solution form

$$u(z,x) = e^{\imath kz} U(x) \qquad v(z,x) = e^{2\imath kz} V(x) \tag{3.34}$$

reduces the above governing equations to the system of ODE's:

$$\frac{1}{2}U'' - kU + UV - (U^2 + 2V^2)U = 0 \tag{3.35}$$

$$\frac{1}{4}V'' - (2k + \beta)V + U^2 - 2(2U^2 + V^2)V = 0 \tag{3.36}$$

3.3.1 Localization of the Linear Spectrum

If embedded solitons exist in equations (3.32), they will do so in a certain parameter regime mandated by the linear spectrum. The linear spectrum is mapped out in the following manner:

$$k < 0 : \quad 2k + \beta > 0 \tag{3.37}$$

u: delocalized v: localized

$$k > 0 : \quad 2k + \beta < 0 \tag{3.38}$$

u: localized v: delocalized

3.3.2 The Variational Approximation

The same technique employed for the type II system will be used. Initially, the two components in the variational ansatz were assumed to have differing widths.

$$U_{core} = A_1 \exp(-\frac{x^2}{{\rho_1}^2}) \tag{3.39}$$

$$V_{core} = A_2 \exp(-\frac{x^2}{{\rho_2}^2}) \tag{3.40}$$

$$\tag{3.41}$$

The delocalized component is modified by adding to the above ansatz the term:

$$U/V_{tail} = a\cos(\kappa x) \tag{3.42}$$

In order to keep the action integral finite, the phase of the delocalized component must take the form (depending on which component is delocalized):

$$U - delocalized: \quad \kappa_u = \sqrt{-2(4k + a^2)} \tag{3.43}$$

$$V - delocalized: \quad \kappa_v = \sqrt{-2(4k + 2\beta + a^2)} \tag{3.44}$$

Varying the action with respect to the parameters yields the following set of E-L equations. (Note that a is taken to be zero after varying L with respect to the respective parameters). Also note that in these equations A_1 corresponds to the core amplitude of the u-component, and A_2 corresponds to the core amplitude of the v-component.

$$A_1: -4\,A_1{A_2}^2\sqrt{\pi}\frac{1}{\sqrt{\frac{2\,{\rho_2}^2+2\,{\rho_1}^2}{{\rho_1}^2{\rho_2}^2}}} - \frac{{A_1}^3\sqrt{\pi}}{\sqrt{{\rho_1}^{-2}}} + 2\,A_1A_2\sqrt{\pi}\frac{1}{\sqrt{\frac{2\,{\rho_2}^2+{\rho_1}^2}{{\rho_1}^2{\rho_2}^2}}} - \frac{k\,A_1\sqrt{2}\sqrt{\pi}}{\sqrt{{\rho_1}^{-2}}} - 1/2\,\frac{A_1\sqrt{2}\sqrt{\pi}}{{\rho_1}^2\sqrt{{\rho_1}^{-2}}} = 0 \tag{3.45}$$

$$\begin{aligned} A_2: \; -4\,{A_1}^2A_2\sqrt{\pi}\frac{1}{\sqrt{\frac{2\,{\rho_2}^2+2\,{\rho_1}^2}{{\rho_1}^2{\rho_2}^2}}} + 1/4\,\frac{(-4\,k\,{\rho_1}^4{\rho_2}^4A_2 - 2\,\beta\,{\rho_1}^4{\rho_2}^4A_2)\,\sqrt{2}\sqrt{\pi}}{{\rho_1}^4{\rho_2}^4\sqrt{{\rho_2}^{-2}}} - \frac{{A_2}^3\sqrt{\pi}}{\sqrt{{\rho_2}^{-2}}} \\ + {A_1}^2\sqrt{\pi}\frac{1}{\sqrt{\frac{2\,{\rho_2}^2+{\rho_1}^2}{{\rho_1}^2{\rho_2}^2}}} - 1/8\,\frac{A_2\sqrt{2}\sqrt{\pi}}{{\rho_2}^2\sqrt{{\rho_2}^{-2}}} = 0 \end{aligned} \tag{3.46}$$

$$\begin{aligned}
\rho_1 \quad : \quad & {A_1}^2 {A_2}^2 \sqrt{\pi} \left(4 \frac{1}{\rho_1 {\rho_2}^2} - 2 \frac{2\,{\rho_2}^2 + 2\,{\rho_1}^2}{{\rho_1}^3 {\rho_2}^2} \right) \left(\frac{2\,{\rho_2}^2 + 2\,{\rho_1}^2}{{\rho_1}^2 {\rho_2}^2} \right)^{-3/2} \\
+ \quad & 1/4 \, \frac{\left(-8\,k\,{\rho_1}^3 {\rho_2}^4 {A_2}^2 - 4\,\beta\,{\rho_1}^3 {\rho_2}^4 {A_2}^2 \right) \sqrt{2}\sqrt{\pi}}{{\rho_1}^4 {\rho_2}^4 \sqrt{{\rho_2}^{-2}}} - \frac{\left(-2\,k\,{\rho_1}^4 {\rho_2}^4 {A_2}^2 - \beta\,{\rho_1}^4 {\rho_2}^4 {A_2}^2 \right) \sqrt{2}\sqrt{\pi}}{{\rho_1}^5 {\rho_2}^4 \sqrt{{\rho_2}^{-2}}} \\
- \quad & 1/4 \, \frac{{A_1}^4 \sqrt{\pi}}{\left({\rho_1}^{-2} \right)^{3/2} {\rho_1}^3} - 1/2 \, {A_1}^2 A_2 \sqrt{\pi} \left(2 \frac{1}{\rho_1 {\rho_2}^2} - 2 \frac{2\,{\rho_2}^2 + {\rho_1}^2}{{\rho_1}^3 {\rho_2}^2} \right) \left(\frac{2\,{\rho_2}^2 + {\rho_1}^2}{{\rho_1}^2 {\rho_2}^2} \right)^{-3/2} \\
- \quad & 1/2 \, \frac{k\,{A_1}^2 \sqrt{2}\sqrt{\pi}}{\left({\rho_1}^{-2} \right)^{3/2} {\rho_1}^3} + 1/2 \, \frac{{A_1}^2 \sqrt{2}\sqrt{\pi}}{{\rho_1}^3 \sqrt{{\rho_1}^{-2}}} - 1/4 \, \frac{{A_1}^2 \sqrt{2}\sqrt{\pi}}{{\rho_1}^5 \left({\rho_1}^{-2} \right)^{3/2}} = 0
\end{aligned} \tag{3.47}$$

$$\begin{aligned}
\rho_2 \quad : \quad & 1/4 \, \frac{\left(-8\,k\,{\rho_1}^4 {\rho_2}^3 {A_2}^2 - 4\,\beta\,{\rho_1}^4 {\rho_2}^3 {A_2}^2 \right) \sqrt{2}\sqrt{\pi}}{{\rho_1}^4 {\rho_2}^4 \sqrt{{\rho_2}^{-2}}} - \frac{\left(-2\,k\,{\rho_1}^4 {\rho_2}^4 {A_2}^2 - \beta\,{\rho_1}^4 {\rho_2}^4 {A_2}^2 \right) \sqrt{2}\sqrt{\pi}}{{\rho_1}^4 {\rho_2}^5 \sqrt{{\rho_2}^{-2}}} \\
+ \quad & 1/4 \, \frac{\left(-2\,k\,{\rho_1}^4 {\rho_2}^4 {A_2}^2 - \beta\,{\rho_1}^4 {\rho_2}^4 {A_2}^2 \right) \sqrt{2}\sqrt{\pi}}{{\rho_1}^4 {\rho_2}^7 \left({\rho_2}^{-2} \right)^{3/2}} - 1/4 \, \frac{{A_2}^4 \sqrt{\pi}}{\left({\rho_2}^{-2} \right)^{3/2} {\rho_2}^3} \\
+ \quad & {A_1}^2 {A_2}^2 \sqrt{\pi} \left(4 \frac{1}{\rho_2 {\rho_1}^2} - 2 \frac{2\,{\rho_2}^2 + 2\,{\rho_1}^2}{{\rho_1}^2 {\rho_2}^3} \right) \left(\frac{2\,{\rho_2}^2 + 2\,{\rho_1}^2}{{\rho_1}^2 {\rho_2}^2} \right)^{-3/2} \\
- \quad & 1/2 \, {A_1}^2 A_2 \sqrt{\pi} \left(4 \frac{1}{\rho_2 {\rho_1}^2} - 2 \frac{2\,{\rho_2}^2 + {\rho_1}^2}{{\rho_1}^2 {\rho_2}^3} \right) \left(\frac{2\,{\rho_2}^2 + {\rho_1}^2}{{\rho_1}^2 {\rho_2}^2} \right)^{-3/2} \\
+ \quad & 1/8 \, \frac{{A_2}^2 \sqrt{2}\sqrt{\pi}}{{\rho_2}^3 \sqrt{{\rho_2}^{-2}}} - 1/16 \, \frac{{A_2}^2 \sqrt{2}\sqrt{\pi}}{{\rho_2}^5 \left({\rho_2}^{-2} \right)^{3/2}} = 0
\end{aligned} \tag{3.48}$$

When u is localized, the fifth E-L equation is

$$\begin{aligned}
a \quad : \quad & -1/4 \, \frac{A_2 \sqrt{\pi} \left(-8\,k - 4\,\beta \right) e^{-1/4 \left(-8\,k - 4\,\beta \right) {\rho_2}^2}}{\sqrt{{\rho_2}^{-2}}} + 1/2 \, \frac{{A_1}^2 \sqrt{\pi}\sqrt{2} e^{-1/8 \left(-8\,k - 4\,\beta \right) {\rho_1}^2}}{\sqrt{{\rho_1}^{-2}}} \\
- \quad & 4\,{A_1}^2 A_2 \sqrt{\pi} e^{-1/4 \, \frac{\left(-8\,k - 4\,\beta \right) {\rho_1}^2 {\rho_2}^2}{2\,{\rho_2}^2 + {\rho_1}^2}} \frac{1}{\sqrt{\frac{2\,{\rho_2}^2 + {\rho_1}^2}{{\rho_1}^2 {\rho_2}^2}}} \\
+ \quad & 1/2 \, \frac{\left(-2\,\beta\,{\rho_1}^4 {\rho_2}^4 A_2 \sqrt{\pi} - 4\,k\,{\rho_1}^4 {\rho_2}^4 A_2 \sqrt{\pi} \right) e^{-1/4 \left(-8\,k - 4\,\beta \right) {\rho_2}^2}}{{\rho_1}^4 {\rho_2}^4 \sqrt{{\rho_2}^{-2}}} \\
- \quad & 2/3 \, \frac{{A_2}^3 \sqrt{\pi}\sqrt{3} e^{-1/12 \left(-8\,k - 4\,\beta \right) {\rho_2}^2}}{\sqrt{{\rho_2}^{-2}}} = 0
\end{aligned} \tag{3.49, 3.50}$$

When v is localized, the fifth E-L equation is

$$\begin{aligned} a \quad : \quad & -4\,{A_2}^2 A_1\sqrt{\pi}e^{1/2\,\frac{k\,{\rho_1}^2{\rho_2}^2}{2\,{\rho_1}^2+{\rho_2}^2}}\frac{1}{\sqrt{\frac{2\,{\rho_1}^2+{\rho_2}^2}{{\rho_2}^2{\rho_1}^2}}} \\ - \quad & 2\,\frac{k\,A_1\sqrt{\pi}e^{1/2\,k\,{\rho_1}^2}}{\sqrt{{\rho_1}^{-2}}}+2\,\frac{k\,A_1\sqrt{\pi}e^{1/2\,k\,{\rho_1}^2}}{{\rho_1}^2\left({\rho_1}^{-2}\right)^{3/2}} \\ + \quad & 2\,A_2A_1\sqrt{\pi}e^{1/2\,\frac{k\,{\rho_1}^2{\rho_2}^2}{{\rho_1}^2+{\rho_2}^2}}\frac{1}{\sqrt{\frac{{\rho_1}^2+{\rho_2}^2}{{\rho_2}^2{\rho_1}^2}}}-2/3\,\frac{{A_1}^3\sqrt{\pi}\sqrt{3}e^{1/6\,k\,{\rho_1}^2}}{\sqrt{{\rho_1}^{-2}}}=0 \end{aligned} \tag{3.51}$$

To reduce the complexity of the above algebraic system, it will be assumed that the widths of the gaussian pulses are equal. Setting $\rho_1 = \rho_2 = \rho$ the reduced Euler-Lagrange equations can be rewritten as follows:

$$A_1^2 = -2A_2^2 + \frac{2\sqrt{3}}{3}A_2 - \sqrt{2}k - \frac{\sqrt{2}}{2\rho^2} \tag{3.52}$$

$$0 = A_2^3 + \left(\frac{\sqrt{2}\beta}{2} + \sqrt{2}k\right)A_2 + \left(2A_2 - \frac{\sqrt{3}}{3}\right)A_1^2 \tag{3.53}$$

$$0 = A_2^4 + \left(2\sqrt{2}k + \sqrt{2}\beta - \frac{\sqrt{2}}{4\rho^2}\right)A_2^2 + \left(2\sqrt{2}k + 4A_2^2 - \frac{4\sqrt{3}}{3}A_2\right)A_1^2 + A_1^4 \tag{3.54}$$

$$0 = 4\sqrt{3}A_2^3 + \left(8\sqrt{3}A_2 - 3\sqrt{2}e^{\frac{1}{12}(4k+2\beta)\rho^2}\right)A_1^2 \tag{3.55}$$

$$0 = 4\sqrt{3}A_2^2 - 3\sqrt{2}A_2e^{-\frac{1}{12}k\rho^2} + 2\sqrt{3}A_1^2 \tag{3.56}$$

The above equations are solved numerically in a similar manner to those in the type II project, with one exception. A technique is employed which allows for a reasonable estimate of a range for the control parameter, A_2. The ODE's (3.36) have a constant of motion given by:

$$\partial_x\left[\frac{1}{4}v_x^2 - (2k+\beta)v^2 - v^4 + u_x^2 - 2ku^2 - u^4 + 2vu^2 - u^2v^2\right] = 0 \tag{3.57}$$

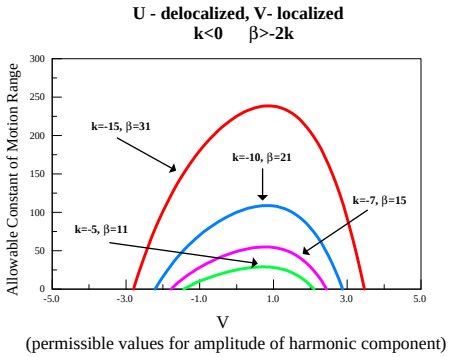

Figure 3.13: allowable values of the control parameter given a point in (β, k) space

The above quantity is constant for any given value (k,β,u,v). From this, it can be shown that

$$\left[U_0^2 - V_0^2 - |k| + \frac{1}{2}V_0^2\right]^2 = -\frac{3}{4}V_0^4 - \frac{1}{2}V_0^3 + \left(1 + \frac{3}{2}|k| - \beta\right)V_0^2 + 2|k|V_0 + k^2 > 0 \quad (3.58)$$

Where U_0 and V_0 are the initial amplitudes of the soliton core. Given a value of k and β, a range of the initial amplitude of the v component can be established. Figure (3.13) shows various ranges of the control parameter used in solving the E-L equations.

Consider the region of the linear spectrum given by $k < 0$, $\beta + 2k > 0$. There were no ES located by the variational approximation. Every crossing of zero which was located corresponds to a region where $\beta + 2k < 0$. Figure (3.14) depicts a number of these numerical results. For the region of the linear spectrum given by $k > 0$, $\beta + 2k < 0$, the variational method did indicate the existence of embedded solitons. Several of these findings in (k, β) space are shown in figure (3.15). It is worth mentioning that the variational approximation returned initial amplitudes for these ES that are quite small (on the order of $< 10^{-1}$). It

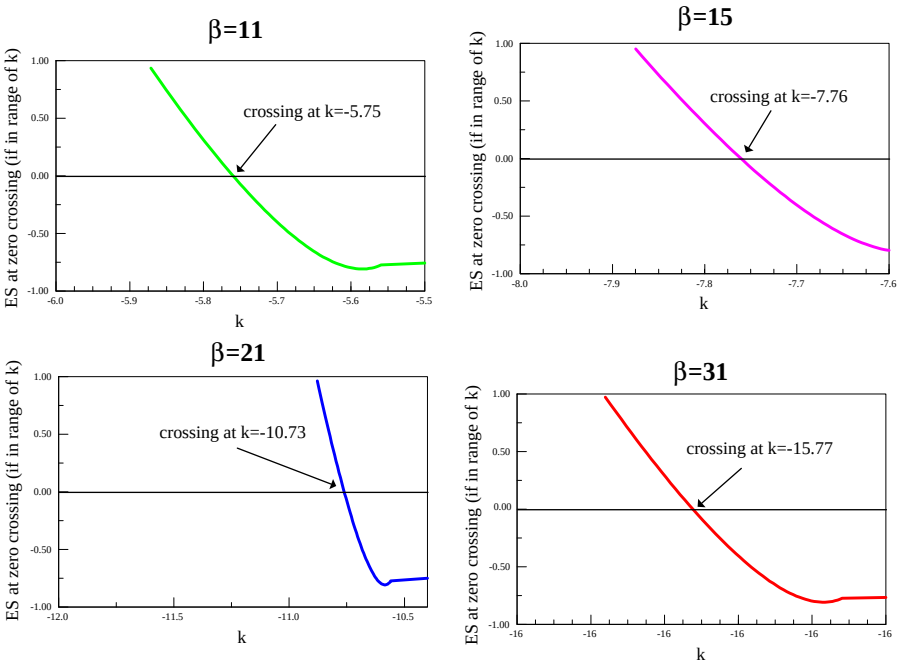

Figure 3.14: numerical results for the variational approximation for the $\chi^{(2)} : \chi^{(3)}$, type I system for $k < 0$

is possible that they do not correspond to ES (these solutions are on the verge of being in the linear regime, where the nonlinear mechanisms which enable the existence of ES fail to dominate).

3.4 Conclusion

In this paper we have demonstrated that there does exist localized solutions to the $\chi^{(2)} : \chi^{(3)}$, Type II optical system for which the propogation constant falls into the continuous spectrum of radiation modes. Figure (3.12) shows in parameter space where such solutions have been found. Additionally, variational results indicate no such structure persists in a $\chi^{(2)} : \chi^{(3)}$, Type I system.

LOCALIZED SOLUTIONS FOR 1D LONGITUDINAL WAVE PROPAGATION IN MICROSTRUCTURED SOLIDS

4.1 Introduction

In recent years, interest in applied research pertaining to microstructured solids has become more prevalent. One such area of interest pertains to what are known as *shape-metal alloys* (SMA). SMA's have potential application in such areas such as aeronautics, development of reconstructive surgical tools, and robotics [8]. Recent work [3] has lead to the realization of the existence of solitary wave solutions in such models. The work done in finding localized solutions was entirely based on numerical integration. This paper examines the use of a variational approximation to find localized ordinary solitons as well as extends the known family of solitons which exist in the SMA model to include *embedded solitons* (ES). Embedded solitons are *localized* solitary wave solutions which exist at discrete points in the continuous spectrum of the linearized system. The accepted model for 1-D longitudinal wave propagation through microstructured media is based on a higher order KdV-type equation. The model (4.1) incorporates third and fifth order dispersion, as well as higher order first and third order nonlinearities.

$$u_t + [P(u)]_x + du_{xxx} + bu_{xxxxx} = 0 \tag{4.1}$$

where the nonlinear potential is given by

$$P(u) = -\frac{1}{2}u^2 + u^4 \tag{4.2}$$

In the above cited paper, the authors numerically solve for solitary wave solutions in the logarithmic parameter range given by

$$0.8 \leq b_l \leq 2.4 \tag{4.3}$$

$$1.4 \leq d_l \leq 4.8 \tag{4.4}$$

For the purposes of the current analysis we will consider the model both in terms of the (b, d) parameter space as stated in equation (4.1) as well as under the transformation determined by (4.5).

$$v(x,t) = \frac{1}{2}u(\sqrt{2|d|}\xi) \qquad \xi = x - ct \tag{4.5}$$

Under this transformation, the stationary state ODE (4.6) governing 1-D longitudinal wave propagation reduces to a 1-dimensional parameter space. (It also scales a coefficient of the nonlinearity).

$$-cv + v_{\xi\xi} + \gamma v_{\xi\xi\xi\xi} - \frac{1}{2}v^2 + \frac{1}{4}v^4 = 0 \tag{4.6}$$

where

$$\gamma = \frac{b}{2d^2} \tag{4.7}$$

4.2 The Linear Spectrum

The search for localized solutions begins with an analysis of the eigenvalues of the linearized spectrum. That is to say, we consider the possible values of the extrinsic parameter, γ, and the wavespeed, c, for which localized solutions (ordinary solitons) may possibly exist. Any localized solution will have a vanishing amplitude for large ξ. Hence, for solitons to exist, all four eigenvalues must remain real. The linear problem has eigenvalues corresponding to

$$\lambda(c;\gamma) = \pm\sqrt{\frac{-1-\sqrt{1-4\gamma c}}{2\gamma}} \quad \sigma(c;\gamma) = \pm\sqrt{\frac{-1+\sqrt{1-4\gamma c}}{2\gamma}} \tag{4.8}$$

To keep all 4 real, it must be that:

$$\gamma < 0 \qquad 0 < \gamma c < \frac{1}{4} \tag{4.9}$$

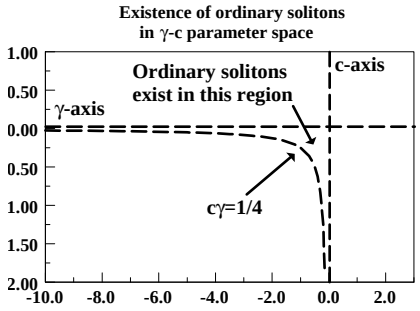

Figure 4.1: the dispersion region (possible values in $c-\gamma$ space) for which localized structure may exist.

If an embedded soliton exists it arises from a saddle-node bifurcation. This is when the stable-unstable manifolds (real roots) correspond to the exponential tails of the embedded

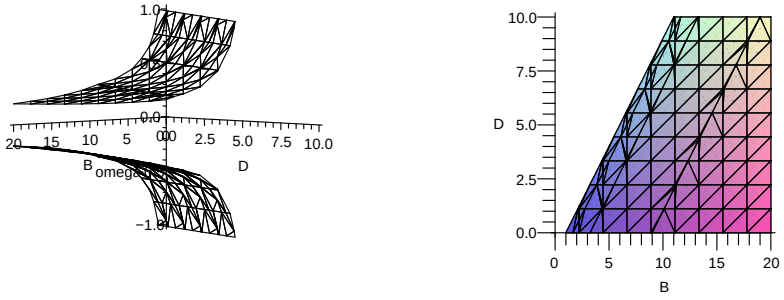

Figure 4.2: the dispersion surface (possible values in (b, d) space) for which ES may exist.

soliton, while the center manifold (imaginary roots) correspond to the continuous wave radiation whose amplitude vanishes [5]. Due to the sensitivity of the existence of embedded solitons with respect to the dispersion coefficients, it is conducive to do the analysis for embedded solitons in terms of the original 2-dimensional parameter space (b, d). In terms of this parameter space, the eigenvalues satisfy the quintic equation for λ given by (4.10). The existence of an embedded soliton necessitates that the only valid parameter region in (b, d) space corresponds to solutions of (4.10) $\omega_1 > 0$ and $\omega_2 < 0$.

$$B\omega^2 - D\omega^2 - 1 = 0 \quad \omega = \lambda^2 \quad B = b/c \quad D = d/c \tag{4.10}$$

Figure (4.2) shows plots for the values in (b, d) space for which embedded solitons may exist. The left figure is a surface plot of (4.10) while the right graphic shows a "top-down" view of the surface. The colored region is the region for which ES may exist. This graphic is more instructive in that it demonstrates the limiting region in (b, d) space for which ES may exist.

4.3 Variational Formulation

4.3.1 The Variational Approximation for Ordinary Solitons

The modality for the variational approximation is quite standard, and is employed throughout many areas of applied mathematics (also known as the Raleigh-Ritz method). The Lagrangian from which equation (4.6) is established is determined by (4.11).

$$L = -\frac{1}{2}cU^2 - \frac{1}{6}U^3 + \frac{1}{20}U^5 - \frac{1}{2}U_\xi^2 + \frac{\gamma}{2}(U_{\xi\xi})^2 \tag{4.11}$$

The search for localized solutions will be facilitated by using a Guassian trial function (4.12).

$$U_{variational} = A\exp(-\frac{\xi^2}{\rho^2}) \tag{4.12}$$

Integrating the Lagrangian density over all space yields the action (4.13)

$$\frac{1}{4}cA^2\sqrt{2}\rho\sqrt{\pi} - \frac{1}{18}A^3\sqrt{3}\rho\sqrt{\pi} + \frac{1}{100}A^5\sqrt{5}\rho\sqrt{\pi} - \frac{1}{4}\frac{A^2\sqrt{2}\sqrt{\pi}}{\rho} + \frac{3}{4}\frac{\gamma A^2\sqrt{2}\sqrt{\pi}}{\rho^3} \tag{4.13}$$

The algebraic constraints for which the variational solution exists can be determined by the associated Euler-Lagrange equations. This is accomplished by varying the action with respect to the core amplitude, A, and the core width, ρ. This algebraic system is given below.

$$30c\sqrt{2}\rho^4 - 10A\sqrt{3}\rho^4 + 3A^3\sqrt{5}\rho^4 - 30\sqrt{2}\rho^2 + 90\gamma\sqrt{2} = 0 \tag{4.14}$$

$$225c\sqrt{2}\rho^4 - 50A\sqrt{3}\rho^4 + 9A^3\sqrt{5}\rho^4 + 225\sqrt{2}\rho^2 - 2025\gamma\sqrt{2} = 0 \tag{4.15}$$

The width of the core can be determined explicitly in terms of the amplitude and wavespeed (4.16). Numerical solution curves of these associated E-L equations are given in figure (1) and figure (2). Using ρ as control parameter, the equations are solved in terms of amplitude (A) and wavespeed (c). The equations are cubic in amplitude, hence there are 3 possible branches of solutions. As the numerics indicate, there are solutions along two of these branches for $0 > \gamma > -1.1$, and only a single branch of solution for $\gamma < -1.1$. Additionally, it is worth mentioning that the variational approximation indicates that localized solutions (at least, for ordinary solitons) only exist for negative core amplitudes. This is was also discovered in the previous work done by *Ilison* and *Salupere* [3].

$$\rho^2 = \frac{-195\sqrt{2} \pm \sqrt{(195\sqrt{2})^2 - 4(255\sqrt{2}c - 60\sqrt{3}A + 12\sqrt{5}A^3)(-1935\sqrt{2}\gamma)}}{2(255\sqrt{2}c - 60\sqrt{3}A + 12\sqrt{5}A^3)} \tag{4.16}$$

4.3.2 The Variational Approximation for Embedded Solitons

The method employed in the identification of embedded solitons in equation (4.1) is modeled after the technique presented in [18]. To locate wave speeds for which there exist embedded solitons, suppose there exists some wave speed, c_{ES} at which an ES exists and within a small neighborhood of c_{ES} there exists a family of delocalized solitons that have a small radiating tail. The tail of such a delocalized soliton will have a form which will be variationally approximated by (4.17). Note that we are interested only in even solutions, hence the use of a *cos* to model the radiating tails. The wavevector $\kappa(c)$ allows for a necessary degree of freedom to ensure convergence of the action.

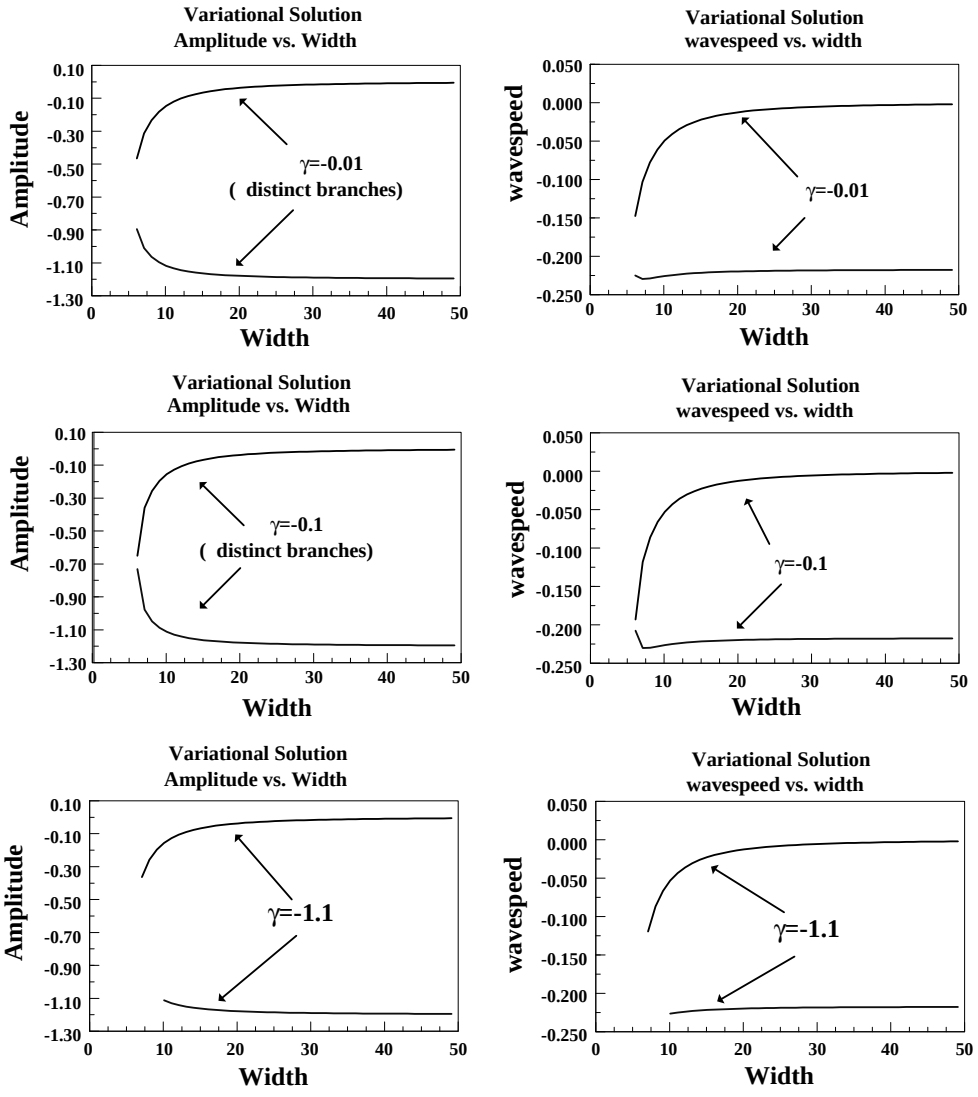

Figure 4.3: variational solution curves beneath the bifurcation point ($\gamma >= -1.1$)

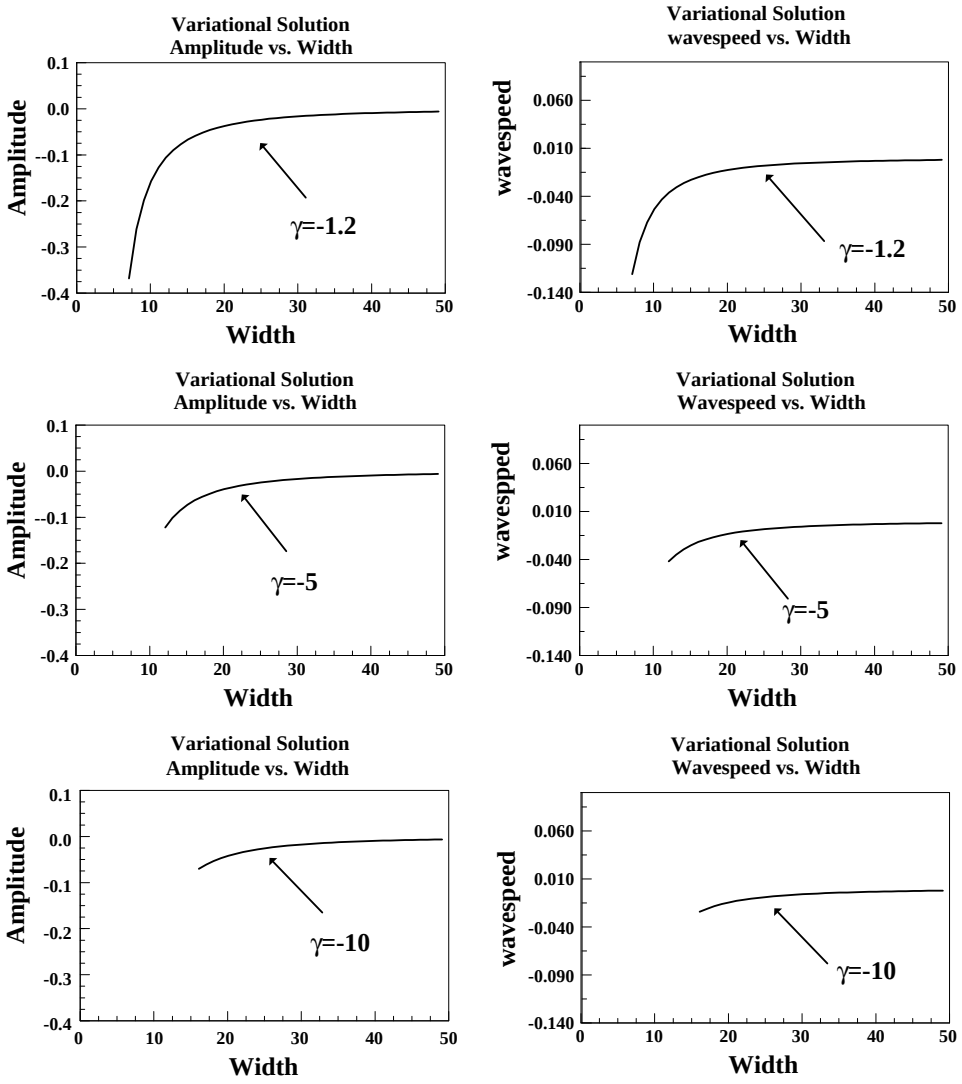

Figure 4.4: variational solution curves beyond the bifurcation point ($\gamma <= -1.2$)

$$U_{tail} = a\cos(\kappa(c)\xi) \tag{4.17}$$

The core of the variational ansatz is taken once again to be a gaussian pulse. The delocalized tail can then be added to the gaussian core to arrive at a reasonable trial given by (4.18).

$$U_{variational} = A\exp(-\frac{\xi^2}{\rho^2}) + acos(\kappa(c)\xi) \tag{4.18}$$

The existence of the action (4.19) depends solely on the appropriate selection of the wavevector. In general, (4.19) does not exist.

$$S(A,\rho,a,c) = \int_{-\infty}^{\infty} L(U = U_{variational})d\xi \tag{4.19}$$

There are terms in $L(U = U_{variational})$ which depend linearly on ξ which is the ultimate cause of the action not existing (in general). Those terms can be annihilated by an appropriate choice for the wave vector (4.20). Of the terms remaining, there those which can be integrated (after using some trigonometric simplification to eliminate higher order radiation cross multiplied with gaussian structure), and terms which are purely radiation.

$$\kappa(c) = \frac{\sqrt{2}}{2}\frac{\sqrt{b(d+\sqrt{d^2+4bc})}}{b} \tag{4.20}$$

The requirement is that the action remain finite, and hence the terms which are pure oscillations are averaged out. The action (up to $O(a^1)$) is then determined by (4.21).

$$
\begin{aligned}
S &= \frac{-A^2\sqrt{\pi}}{1800\rho^3}[450\sqrt{2}c\rho^4 + 100\sqrt{3}A\rho^4 - 18\sqrt{5}A^3\rho^4 + 450\sqrt{2}d\rho^2 - 1350\sqrt{2}b \\
&- 225A^2a\rho^4\exp(-\phi) + 450\sqrt{2}a\rho^4\exp(-2\phi)] + O(a^2) \qquad (4.21)
\end{aligned}
$$

where

$$
\phi = \frac{1}{32}\frac{(d + \sqrt{d^2 + 4bc})}{b}\rho^2 \qquad (4.22)
$$

To approximate the wave speeds (c) for which embedded solitons exist, we will consider an approximation for which the delocalized solitons have a small oscillating amplitude. The action is varied with respect to the core amplitude (A), the width of the core (ρ), and the small radiating amplitude (a). The resulting E-L equations are then evaluated at the condition $a = 0$. That is, we consider the variation of the action with respect to those terms which are linear in the radiating amplitude.

$$
\begin{aligned}
(\frac{\partial S}{\partial A}|_{a=0} = 0) \quad &: \quad -30\sqrt{2}c\rho^4 - 10\sqrt{3}A\rho^4 + 3\sqrt{5}A^3\rho^4 \\
&- \quad 30\sqrt{2}d\rho^2 + 90\sqrt{2}b = 0 \qquad (4.23) \\
(\frac{\partial S}{\partial \rho}|_{a=0} = 0) \quad &: \quad 225\sqrt{2}c\rho^4 + 50\sqrt{3}A\rho^4 - 9\sqrt{5}A^3\rho^4 \\
&- \quad 225\sqrt{2}d\rho^2 + 2025\sqrt{2}b = 0 \qquad (4.24) \\
(\frac{\partial S}{\partial a}|_{a=0} = 0) \quad &: \quad \exp(-\phi)(2\sqrt{2}\exp(-\phi) - A^2) = 0 \qquad (4.25)
\end{aligned}
$$

Figures (4.5)-(4.10) show numerical solution curves for the algebraic set of E-L equations (4.23)-(4.25). Note that these solution curves are in terms of the (b, d) parameter space (with

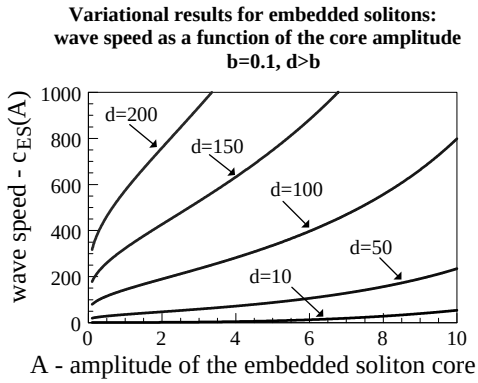

Figure 4.5: c_{ES}(A) for $d > b$, $b = 0.1$

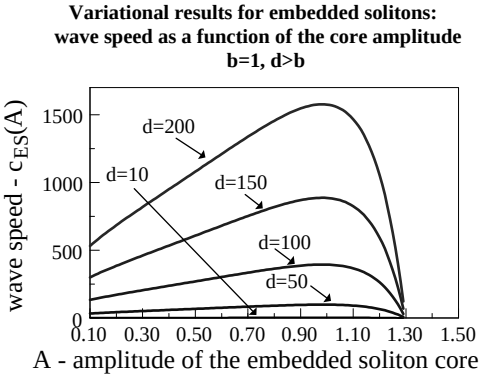

Figure 4.6: c_{ES}(A) for $d > b$, $b = 1$

respect to the original posturing of the dynamical system). The following section offers a discussion of these variational results.

4.3.3 Summary of Variational Results for Embedded Solitons

In the area of the parameter space for which the third order dispersion dominates the fifth order dispersion (i.e., $d > b$), parameter estimates for embedded solitons are readily available. Figures (4.5) through (4.8) represent parameter curves along which embedded solitons exist

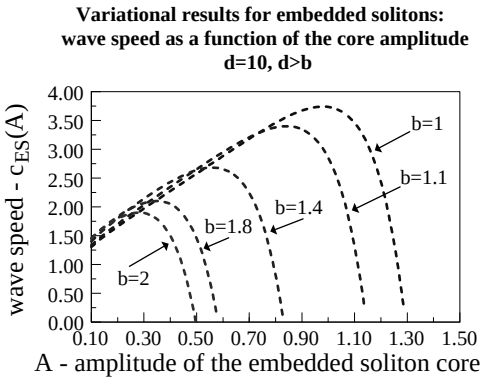

Figure 4.7: c_{ES}(A) for $d > b$, b near unity

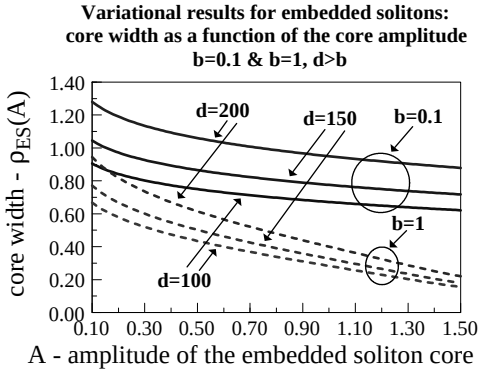

Figure 4.8: ρ_{ES}(A) for $d > b$, solid line: $b = 0.1$, dashed line: $b = 1$

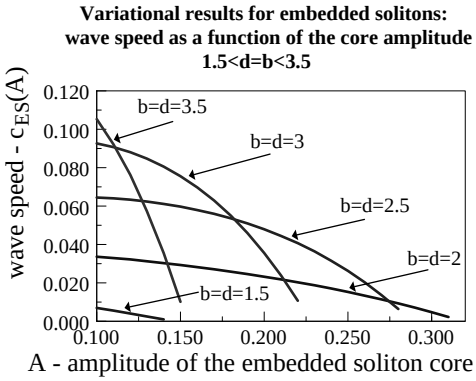

Figure 4.9: $c_{ES}(\mathrm{A})$ for $d = b$

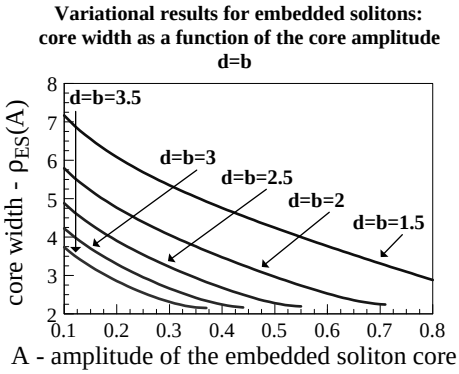

Figure 4.10: $\rho_{ES}(\mathrm{A})$ for $d = b$

for this region of (b, d)-space. In order to locate these parameter curves, it is necessary to keep b of order unity or less. In fact, is required that b remain in the approximate interval $b \in (0, 2.6)$. The third order dispersion can vary up to a couple orders of magnitude greater than b, and the parameter curves still persist. Figure (4.5) depicts the required wave speed as a function of the core amplitude of the embedded soliton for $b = 0.1$. As the fifth order dispersion is increased in value, the viable amplitude range which support positive wave speeds (required by the spectral configuration) drops dramatically. This is illustrated in Figure (4.6). This trend continues as $b \to 2.6$ (roughly). If b is increased beyond this value, the variational approximation returns wave speeds which are negative for all values of A. This is illustrated in Figure (4.7). In Figure (4.7), the third order dispersion is fixed at one order of magnitude, and b is varied between $b = 1$ and $b = 2$. As $b \to 2$, the wave speed goes through a zero at relatively small amplitudes. As previously indicated, at about $b \approx 2.6$, the approximation produces nothing but negative wave speeds. Figure (4.8) gives parameter estimates for the core width, ρ, as a function of the core amplitude. The figure contains three values of the third order dispersion ($d = 100$, $d = 150$, and $d = 200$) for two different values of the fifth order dispersion ($b = 0.1$ and $b = 1$). As expected, the width of the embedded soliton decreases with larger amplitudes. Additionally, as b becomes more dominant, the width estimate for the embedded soliton core is suppressed.

Another area in (b, d) parameter space which the variational approximation predicts the existence of embedded solitons is when the third and fifth order dispersions are comparable in magnitude. For this configuration of the parameter space, there is a limited region in which existence curves persist. Most of the numerical analysis for this case yielded a negative

wave number (which defies the required configuration of the linear spectrum). Figures (4.9) and (4.10) show embedded soliton parameter curves for $b = d$. The parameter values for embedded solitons were located in the region $0.8 < b = d < 3.9$.

In the case of the fifth order dispersion dominating the third order dispersion, no numerical predictions for embedded solitons were located. For this case ($b > d$), the associated wave speeds returned by the variational approximation are found to be complex.

It is worth mentioning that negative values for the dispersion coefficients were tested. In this case, no embedded solitons are located by the variational approximation. If b is taken to be negative (regardless of the sign of d), all predicted wave speeds become complex. If d is taken to be negative (with b positive), only negative wave speeds are recovered. This does not meet the requirement of the linear spectrum.

4.4 Numerical Validation

4.4.1 Determination of Γ at $\xi = 0$.

Since only even solutions are being considered, numerical integration of equation (4.6) requires knowledge of two things. The first of these is the core amplitude, which may be obtained from the variational estimate. The next piece of required information is the value of the second derivative at the origin (assuming the integration is taken from the origin to infinity). To obtain a representation for the curvature at the origin ($U(\xi = 0) = \Gamma$), in terms of known quantities, consider the following constant of motion. Multiplying the aforementioned equation by U_ξ and integrating yields:

$$\frac{d}{d\xi}\left[\frac{1}{2}cU^2 - \frac{1}{6}U^3 + \frac{1}{20}U^5 + \frac{1}{2}(U_\xi)^2 + \gamma U_{\xi\xi\xi}U_\xi - \frac{\gamma}{2}(U_{\xi\xi})^2\right] = 0 \tag{4.26}$$

Hence, at the origin, the initial amplitude and curvature are related by:

$$\Gamma^2 = \frac{1}{\gamma}\left(cA^2 - \frac{1}{3}A^3 + \frac{1}{10}A^5\right) \tag{4.27}$$

4.4.2 Results of Numerical Integration

Numerical integration of equation (4.6) was facilitated by a modified Runge-Kutta routine which could search out for localized structure. The routine accomplishes this feat by integrating out to a certain point, determines the behavior of the eigenmodes (in this case, four of them), extrapolates back to the origin and establishes a manner in which to change a degree of freedom (i.e., the initial amplitude or curvature) in such a way as to find the localized structure. For the case of the embedded soliton, regions (b, d) for which variational solutions were found corresponded to regions for which there were delocalized solitons. The delocalized solitons exit for a continuous interval of wavespeed values. Varying the wavespeed and tracking where the amplitude of the delocalized radiation dies off yields a numerical validation of the existence of an embedded soliton. It is worth noting that there are cases in which the amplitude of the radiation simply *approaches* zero, and does not actually become zero. To ensure this is not the case, the values of the complex eigenmodes (note that for the ES there are two real and two complex eigenmodes) are tracked through phase shift of π. This phase transition indicates the delocalized amplitude *actually goes through a zero*. Figures (4.11)-(4.13) Show the results of the numerical integration. The near-localized solution is

superimposed with the nearby member of the delocalized soliton family.

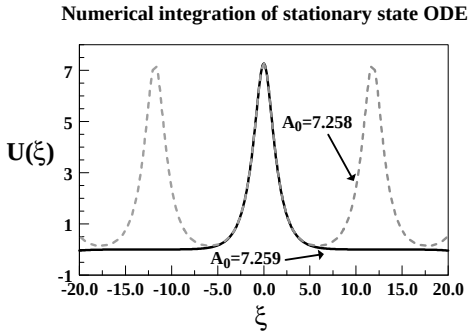

Figure 4.11: $b = 0.1$, $d = 50$, $c = 35.7$, $\Gamma = -8.284195797$

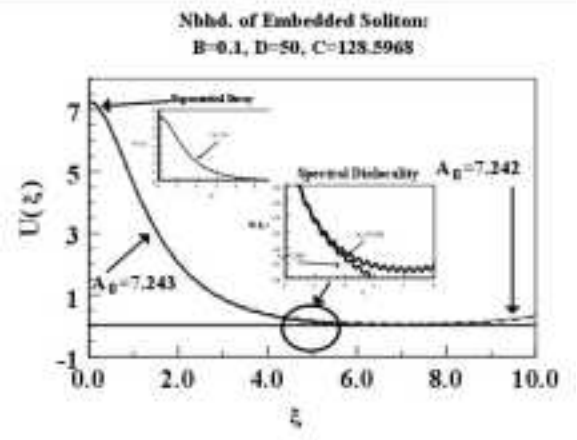

Figure 4.12: numerical integration of equation in (b, d) space

4.5 Conclusion

In this paper we have demonstrated that there does exist localized solutions to equation (4.1) as initially investigated by *Ilison* and *Salupereit* in early 2004 [3]. Beyond ordinary solitons, there also exist *embedded solitons*. Both types of solution structure can be readily

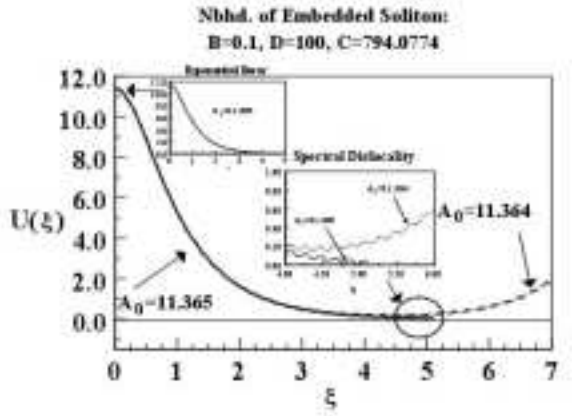

Figure 4.13: numerical integration of equation in (b, d) space

identified using a variational approximation.

LIST OF REFERENCES

[1] *http://www-history.mcs.st-andrews.ac.uk/Biograpihies/Lagrange.html.*

[2] Soliton Perturbations: A Variational Principle for the Soliton Parameters. *Physica Scripta*, 20:479–485, 1979.

[3] George B. Arfken and Hans J. Weber. *Mathematical Methods for Physicsts.* Academic Press, 1995.

[4] W.W. Rouse Ball. *A Short Account of the History of Mathematics.* Martino Publishing, 2004.

[5] A.R. Champneys. Codimension-one persistence beyond all orders of homoclinic orbits to singular saddle centres in reversible systems. *Nonlinearity*, 14:87–112, 2001.

[6] A.R. Champneys, J. B.A. Malomed, and D.J. Kaup Yang. Embedded Solitons: solitary waves in resonance with the linear spectrum. *Physica D*, 152-153:340–354, 2001.

[7] Min Chen, D.J. Kaup, and Boris A. Malomed. Three-Wave Solitons and Continuous Waves in Media with Competing Quadratic and Cubic Nonlinearities. *Phys. Rev. E*, 69:056605, 2004.

[8] Ivan Christov. *Wavelet-Galerkin Methods for Partial Differential Equations.* Massachusetts Institute of Technology Matrix Analysis and Wavelets REU, TAMU, 2003.

[9] Gardner C.S., Greene J.M., and M.D. Kruskal. Method for solving the Korteweg-de Vries equation. *Phys. Rev. Lett.*, 19:1095–1097, 1967.

[10] Lawrence C. Evans. *Partial Differential Equations*. AMS Graduate Studies in Mathematics, 1998.

[11] William R. Hamilton. On a General Method in Dynamics. *Philosophical Transactions of the Royal Society of London*, II:247–308, 1834.

[12] William R. Hamilton. Second Essay on a General Method in Dynamics. *Philosophical Transactions of the Royal Society of London*, I:247–308, 1835.

[13] Homer. *Aeneid*. Vintage Press, 1996.

[14] D.J. Kaup. Variational Solutions for the Discrete Nonlinear Schrodinger Equation. *Mathematics and Computers in Simulation*, 69:322–333, 2005.

[15] D.J. Kaup and T.I. Lakoba. Variational Method: How It Can Generate False Instabilities. *J. Math. Phys.*, 37:3442–62, 1996.

[16] D.J. Kaup and B.A. Malomed. The variational principle for nonlinear waves in dissipative systems. *Physica D*, 87:155–159, 1995.

[17] D.J. Kaup and Boris A. Malomed. Variational Principle for the Zakharov-Shabat equations. *Physica D*, 84:319–328, 1995.

[18] D.J. Kaup and Boris A. Malomed. Embedded Solitons in Lagrangain and Semi-Lagrangian Systems. *Physica D*, 184:153–161, 2003.

[19] D.J. Kaup and Gary E. Thomas. Variational Principle for Cross-Field Devices. *J. Plasma Physics*, 57:765–84, 1997.

[20] D.J. Kaup and T.K. Vogel. Quantitative Measurement of Variational Approximations. *Physics Letters A*, 362:289–297, 2007.

[21] Don S. Lemons. *Perfect Form*. Princeton University Press, 1997.

[22] Christian Lubich. On Variational Approximations in Quantum Molecular Dynamics. *Mathematics of Computation*, 74:765–779, 2005.

[23] D. Mihalache, D. Mazilu, L.C. Crasovan, I. Towers, B.A. Malomed, A.V. Buryak, L. Tornernd, and F. Lederer. Stable three-dimensional spinning optical solitons supported by competing quadratic and cubic nonlinearities. *Physical Review E*, 74:047601, 2006.

[24] Phillip M. Morse and Herman Feshbach. *Methods of Theoretical Physics, Part II*. McGraw-Hill, New York, 1953.

[25] Robert K. Nesbet. *Variational Principles and Methods in Theoretical Physics and Chemsitry*. Cambridge University Press, 2003.

[26] Isaac Newton. *Principia*. Prometheus Books UK, 1995.

[27] Gerald Rosen. *Formulations of Classical and Quantum Dynamical Theory*. Academic Press, New York, 1969.

[28] Jakob Steiner. *Gesammelte Werke*. Prussian Academy of Sciences, 1881.

[29] Jonathan A D Wattis. Variational approximations to breathers in the discrete sine-Gordon equation II: moving breathers and Peierls-Nabarro energies. *Nonlinearity*, 9:1583–1598, 1996.